Taylor & Francis
Taylor & Francis Group

ORIGINAL RESEARCH

🔓 OPEN ACCESS ✓ Check for updates

CD161+CD127+CD8+ T cell subsets can predict the efficacy of anti-PD-1 immunotherapy in non-small cell lung cancer with diabetes mellitus

Jingjing Qu [ID][a,b]*, Yuekang Li[a,b]*, Binggen Wu[a,b], Qian Shen[a,b], Lijun Chen[c], Wenjia Sun[a,b], Bo Wang[d], Lixiong Ying[d], Li Wu[e], Hong Zhou[a], Jianya Zhou[a,b], and Jianying Zhou[a,b]

[a]Department of Respiratory Disease, Thoracic Disease Center, The First Affiliated Hospital, Zhejiang University School of Medicine, Hangzhou, Zhejiang, P. R. China; [b]The Clinical Research Center for Respiratory Diseases of Zhejiang Province, Hangzhou, Zhejiang, P. R. China; [c]State Key Laboratory for Diagnosis and Treatment of Infectious Diseases, National Clinical Research Center for Infectious Diseases, The First Affiliated Hospital, Zhejiang University School of Medicine, Hangzhou, Zhejiang, P.R. China; [d]Department of Pathology, The First Affiliated Hospital, Zhejiang University School of Medicine, Hangzhou, Zhejiang, P. R. China; [e]Department of Endocrinology, The First Affiliated Hospital, Zhejiang University School of Medicine, Hangzhou, Zhejiang, P. R. China

ABSTRACT
The role of CD161+CD127+CD8+ T cells in non-small cell lung cancer (NSCLC) patients with diabetes remains unexplored. This study determined the prevalence, phenotype, and function of CD8+ T cell subsets in NSCLC with diabetes. We recruited NSCLC patients ($n = 436$) treated with anti-PD-1 immunotherapy as first-line treatment. The progression-free survival (PFS), overall survival (OS), T cells infiltration, and peripheral blood immunological characteristics were analyzed in NSCLC patients with or without diabetes. NSCLC patients with diabetes exhibited shorter PFS and OS ($p = 0.0069$ and $p = 0.012$, respectively) and significantly lower CD8+ T cells infiltration. Mass cytometry by time-of-flight (CyTOF) showed a higher percentage of CD161+CD127+CD8+ T cells among CD8+T cells in NSCLC with diabetes before anti-PD-1 treatment ($p = 0.0071$) than that in NSCLC without diabetes and this trend continued after anti-PD-1 treatment ($p = 0.0393$). Flow cytometry and multiple-immunofluorescence confirmed that NSCLC with diabetes had significantly higher CD161+CD127+CD8+ T cells to CD8+T cells ratios than NSCLC patients without diabetes. The RNA-sequencing analysis revealed immune-cytotoxic genes were reduced in the CD161+CD127+CD8+ T cell subset compared to CD161+CD127-CD8+ T cells in NSCLC with diabetes. CD161+CD127+CD8+ T cells exhibited more T cell-exhausted phenotypes in NSCLC with diabetes. NSCLC patients with diabetes with ≥ 6.3% CD161+CD127+CD8+ T cells to CD8+T cells ratios showed worse PFS. These findings indicate that diabetes is a risk factor for NSCLC patients who undergo anti-PD-1 immunotherapy.CD161+CD127+CD8+ T cells could be a key indicator of a poor prognosis in NSCLC with diabetes. Our findings would help in advancing anti-PD-1 therapy in NSCLC patients with diabetes.

Introduction

According to GLOBOCAN 2020, lung cancer is the leading cause of cancer-related death, with an age-standardized rate of cancer mortality of 30.2 per 100,000 population.[1] The number of new cases of lung cancer in China has continued to rise, and non-small cell lung cancer (NSCLC) accounts for 80–85% of all lung cancer cases.[2,3] As our understanding of tumor immunity has increased, immunotherapy has become a conventional treatment for NSCLC.[4–6] In recent years, the application of anti-programmed cell death protein 1 (PD-1), anti-programmed cell death protein ligand 1 (PD-L1) and cytotoxic T lymphocyte antigen-4 (CTLA-4) to advanced NSCLC patients with nonsensitive gene mutations has received widespread attention in immuno-oncology.[7–9]

Diabetes mellitus (DM) is associated with significant mortality and comorbidities, including cardiovascular disease, kidney disease, retinopathy, peripheral vascular disease, and neuropathy.[10–12] DM is also related to the increased incidence and mortality of several cancers, such as colorectal, prostate, breast, and pancreatic cancers.[13] Furthermore, patients with DM-related cancer and poor glycemic control have poor long-term clinical outcomes and survival rates.[14] The mechanism underlying high sugar-induced cancer aggressiveness differs among different cancer types. Glucose can activate many signaling pathways, including extracellular signal-regulated kinase (ERK), signal transducer and activator of transcription (STAT)-3, and nuclear factor (NF)-κB, which are involved in cancer cell proliferation, metastasis, and resistance to chemotherapy.[15–17] The activation of these intracellular pathways regulates the transcription of specific downstream targeting elements and promotes tumor aggressiveness. Therefore, DM has been identified as an indicator of cancer progression.[18]

The number of patients with both DM and lung cancer has been increasing annually. DM is considered an independent

prognostic factor for overall survival (OS) in patients with DM and NSCLC who receive a standard treatment.[19] The tumor microenvironment of NSCLC is important for its progression and metastasis. Interestingly, the infiltration of immune cells, especially T cells, into the tumor microenvironment is linked to the metabolic features of tumors that are important for therapeutic strategies.[20,21] Glucose metabolism is pivotal to the proliferation, differentiation, and effect of various immune cells in changing the tumor microenvironment.[22,23] The impaired anti-tumor activity of γδ T cells due to dysglycemia may lead to the occurrence of cancer in patients with diabetes.[24] Hyperglycemia induces the M2 polarization of tumor-associated macrophages and reduces anti-tumor immunity.[25] Furthermore, hyperglycemia can impair the expression of granulocyte colony-stimulating factors, thus impeding the mobilization of anti-tumor neutrophils and increasing tumor metastatic burden.[26] Metformin, a type 2 DM drug, can attenuate CD4+CD25+ regulatory T cells in the tumor microenvironment, which is related to the mechanistic targeting of rapamycin complex 1 (mTORC1) activation and metabolic reprogramming toward glycolysis.[27] Recently, researchers have developed a method for obtaining comprehensive immune cells from peripheral blood.[28,29] However, to the best of our knowledge, no studies have focused on the characteristics of infiltrating immune cells using mass cytometry by time-of-flight (CyTOF) in NSCLC patients with diabetes.

In the present study, we examined a possible link between DM and immune cell infiltration in patients with NSCLC. Differences in tumor microenvironment profiles were compared between NSCLC patients with and without diabetes using CyTOF to explain the poor progression-free survival (PFS) and OS observed in NSCLC patients with diabetes. Furthermore, we determined the prevalence, phenotype, and function of CD8+ T cell subsets defined by the expression of CD161 and CD127 in NSCLC with diabetes. Our findings demonstrate for the first time that these CD8+ T subsets have prognostic relevance in NSCLC with diabetes.

Materials and methods

Study design and patients

We recruited patients with NSCLC treated with anti-PD-1 immunotherapy from the Department of Respiratory Disease, First Affiliated Hospital, Zhejiang University School of Medicine, between November 2018 and December 2021 in the retrospective cohort. The study was conducted in accordance with the Declaration of Helsinki and approved by the Ethics Committee of The First Affiliated Hospital of Zhejiang University School of Medicine (Approval No. 2023–0343). The performance status of patients before anti-immunotherapy was evaluated using the Eastern Cooperative Oncology Group (ECOG) performance scale. Patient recruitment for the retrospective and validation cohorts included in this study adhered to the following inclusion and exclusion criteria: patients were included if they had been diagnosed with locally advanced or metastatic NSCLC based on histological or cytological analysis, had received at least two courses of treatment of immune checkpoint inhibitors (ICIs) therapy, or had a performance status of 0–1 and no organ dysfunction. All patients received anti-PD-1 therapy as the first-line

treatment. Patients were excluded if they had an ECOG score of ≥ 2, had received anti-PD-1 therapy as second-line treatment or later, or had sensitive driver gene mutations, such as epidermal growth factor receptor (EGFR) mutations, ROS1 rearrangement, and anaplastic lymphoma kinase (ALK)-positive NSCLC. Patients with serious adverse events, who discontinued treatment due to adverse events, or who received < 2 cycles of immunotherapy were also excluded. The included patients were separated into two groups: NSCLC patients with diabetes and without diabetes. To evaluate the treatment efficacy, collected patient information included demographics, clinical characteristics, treatment information, and other relevant data, including the date of disease progression or death.

The primary outcomes of this study were the objective response rate (ORR), PFS, and OS. The ORR is the percentage of patients who achieved complete response/partial response as determined by an investigator, based on the Response Evaluation Criteria in Solid Tumors, version 1.1.[30] OS was defined as the time from the initiation of ICIs administration to death for any reason or to the final follow-up. PFS was defined as the time from the initiation of ICIs administration to first sign of disease progression or death from any cause.

Animal model

Six-week-old C57BL/6J male mice were purchased from Hangzhou Medical College (Hangzhou, China). All animal experimental procedures were approved by the Ethics Review Committee of the Experimental Animal Center of Zhejiang University School of Medicine (ethical approval number: 2023–974). C57BL/6J mice were fasted for 12 h and then intraperitoneally (i.p.) injected with 180 mg/kg body weight streptozotocin (STZ; S0130, Sigma-Aldrich, Darmstadt, Germany), which was dissolved in 0.05 M citrate buffer. The control group received the citrate buffer at the same volume. The concentration of blood glucose (≥12 mmol/L) in the mice was verified for the DM model. Each mouse was injected subcutaneously with 5×10^5 Lewis lung cancer cells. When the tumor had grown to 50 mm³, the anti-mouse-PD-1 mAb (BioXcell, Cat#BE0146, New Hampshire, USA) or IgG isotype control (BioXcell, Cat#BE0089) was injected intraperitoneally into the mice for therapeutic treatment (every 2 days, three times in total, 10 μg/g anti-PD-1 per mouse). The tumor was checked using a digital caliper, and the tumor volume was calculated using the following formula: tumor volume = (width² × length)/2.

Peripheral blood mononuclear cell isolation

To collect peripheral blood mononuclear cells (PBMCs), 5 mL fresh blood was collected from each patient before anti-PD-1 therapy and after one cycle of anti-PD-1 treatment. PBMCs were separated from whole blood through density and gradient centrifugation using Ficoll referred by the previous study.[31] PBMCs were washed and resuspended in pre-cooled fluorescence activated cell sorting (FACS) buffer [1× phosphate buffered saline (PBS) along with 0.5% bovine serum albumin (BSA)], and they were centrifuged at 400 × g for 5 min at 4°C. The cells were counted with a hemocytometer, and more than

3×10^6 cells were ready for further staining. The viability rate was > 85%.

CyTOF preparation and data analysis

The antibody combination contained 42 antibodies involved in various immune subpopulations. Information on clone number, company, and catalog number is shown in Supplementary Table S1, including antibody labeling with the indicated mass tag, which was used according to the Maxpar antibody conjugation kit (Fluidigm, San Francisco, CA, USA). The cells were washed with $1 \times$ PBS and stained with 100 µL of 250 nM cisplatin (Fluidigm) for 5 min. They were then incubated in an Fc receptor blocking solution before staining with a surface antibody cocktail for 30 min on ice. Then the cells were washed three times with FACS buffer (including $1 \times$ PBS + 0.5% BSA), centrifuged at $800 \times g$ and 4°C for 5 min. The supernatant was discarded. The cells were fixed with 200 µL intercalation solution (Maxpar Fix and Perm Buffer containing 250 nM 191/193Ir, Fluidigm) overnight (~8–16 h). After fixation, the cells were washed once with FACS buffer and then with Perm Buffer (eBioscience, San Diego, CA, USA), stained with an intracellular antibody cocktail for 30 min. Subsequently, the cells were rinsed with FACS buffer and incubated in 1× PBS on ice for 20 min with a barcode. Then, the cells were washed, resuspended in deionized water with 20% EQ beads (Fluidigm), and evaluated using a mass cytometer (Helios, Fluidigm, USA). Samples were sent to PLTTECH (Hangzhou, China), who conducted the CyTOF experiments.[28] Before loading each batch of samples, the instrument adjusted the signaling intensity of each channel to maintain the same bead signal (140Ce, 151Eu, 153E u, 165Ho, and 175 Lu).

The FCS data for each sample were debarcoded from the raw data according to a doublet-filtering scheme based on special mass-tagged barcodes.[32] The FCS files from different batches were standardized using bead normalization.[33] Following data standardization, debris, dead cells, and doublets were manually removed using the FlowJo software, leaving single live immune cells. We used the PhenoGraph clustering algorithm[34] to cluster all cells according to the marker expression level in single cells, adjust the clustering parameters to obtain an appropriate number of cell subpopulations, and annotate the cell types of each cluster via the marker gene expression profiles on a heatmap of clusters. Meanwhile, the dimensionality reduction algorithm, t-distributed stochastic neighbor embedding, was applied to visualize the high-dimensional data in two dimensions to indicate the distribution of each cluster on a two-dimensional graph and the expression of each marker or sample type.[35]

Multiplex immunohistochemistry/immunofluorescence

Paraffin sections were obtained from the Department of Respiratory Disease, Thoracic Disease Center, First Affiliated Hospital, Zhejiang University School of Medicine for immunostaining. Immunostaining was performed according to a previous study, using the primary antibodies CD3 (17617–1-

AP, Proteintech; 1:200) and CD8 (Ab237709, Abcam; 1:200).[31,36] The immunostained tissue sections were checked and counted under a microscope (Olympus BX53, Japan). Each sample was counted separately by at least two pathologists and examined until a consensus was reached.

Multiplex immunofluorescence staining was performed using the Opal Polaris 7 Color Multiplex IHC kit (NEL861001KT, Akoya Biosciences, Delaware, USA). The slides were dewaxed and antigenic repair was performed using EDTA buffer (pH 9.0). The slides were washed with 3% H_2O_2 for 15 min and sealed with 3% BSA (B2064-100 G, Sigma-Aldrich). The slides were then incubated with primary antibodies against CD3 (17617–1-AP, Proteintech; 1:1000), CD8 (Ab237709, Abcam; 1:2000), CD161 (Ab302564, Abcam; 1:300), CD127 (Ab180521, Abcam; 1:50), CD57 (72031, Cell Signaling Technology; 1:300), and GZMB (13588–1-AP, Proteintech; 1:50), followed by Opal Polymer HRP Ms+Rb (Akoya Biosciences). The samples were subjected to optical fluorophore-conjugated tyramide signal amplification (Akoya Biosciences). The dyes used to detect each antibody were Opal 570 dye (CD3), Opal 520 dye (CD8), Opal 690 dye (CD161), Opal 620 dye (CD57 or CD127) and Opal 480 (GZMB). These steps were repeated until cells were labeled with the expected markers and 4',6-diamidino-2-phenylindole. Slices were visualized using the Vectra Polaris Quantitative Pathological Imaging System (Akoya Biosciences) and analyzed using the InForm software (Akoya Biosciences).

Flow cytometry

PBMCs were isolated using Ficoll (Cytiva)-based density gradient centrifugation according to the manufacturer's instructions. For flow cytometric analysis, PBMC samples were pretreated with human IgG blocker (BioLegend, Cat#422302) for 20 min. Then, the cells were washed thrice with FACS buffer (including 1× PBS + 0.5% BSA) and centrifuged at $800 \times g$ and 4°C for 5 min. All flow cytometry antibodies were purchased from BioLegend (San Diego, CA, USA). We used phytohemagglutinin (PHA, Dakewe, Cat#2030411) to stimulate T cells. PBMCs were incubated with the following antibody conjugates on ice in the dark: APC/Cyanine 7-CD3 (Cat#300425), PerCP/Cyanine 5.5-CD8a (Cat#301031), PE-CD57 (Cat#393307), APC-CD127 (Cat#351315), FITC-granzyme B (GZMB) (Cat#515403), and PE/Cyanine7-CD161 (Cat#339917), PE-granulysin (GNLY) (Cat#348003), PE-LAG3 (Cat#369305), FITC-KLRG1 (Cat#367713), PE-TIGIT (Cat#372703), and FITC-PD-1 (Cat#329903). All cell surface reactions (CD3, CD8, CD57, CD127, CD161, KLRG1, TIGIT, LAG3, and PD-1) were performed at 4°C for 30 min. The permeabilization step that allowed for intracellular staining (GZMB and GNLY) was performed according to the manufacturer's protocol (BioLegend, Cat#426803). Finally, the cells were resuspended in 300 µL FACS buffer. Flow cytometric analysis was performed using a BD FACS Fortessa multicolor flow cytometer (BD Biosciences). For the mouse model flow cytometry test, the samples were subjected to flow cytometry analysis following staining with surface markers APC-CD127 (Cat#135011, BioLegend), PerCP/Cyanine5.5-CD3(Cat#100327,BioLegend), APC/

Cyanine7-CD8a (Cat#100713, BioLegend), and FITC-CD161 (Cat#108705, BioLegend). The data were further analyzed with FlowJo vX.07 software (Tree Star).

RNA-sequencing

For mRNA sequencing, RNA samples were prepared using the TruSeq RNA Sample Preparation according to the manufacturer's instructions and performed by GENEWIZ from Azenta Life Sciences (Suzhou, China). Briefly, the poly-A-containing mRNA molecules were purified from total RNA using poly-T oligo-attached magnetic beads. The cleaved RNA fragments were then reverse transcribed into first-strand cDNA (complementary DNA) using random hexamers, followed by second-strand cDNA synthesis. The cDNA fragments were purified, end blunted, "A" tailed, and adaptor ligated. Polymerase chain reaction (PCR) was used to selectively enrich DNA fragments with adapter molecules on both ends and amplify the amount of DNA in the library. The library was qualified using an Agilent 2100 bioanalyzer and quantified using Qubit and qPCR. The produced libraries were sequenced on the HiSeq 2500 platform, and differential expression analysis was performed using DESeq2. Significant differentially expressed genes (DEGs) were defined as having a Q value < 0.05. The expression patterns of genes among different groups and samples were determined using hierarchical cluster analysis of DEGs in the R software.

Statistical analysis

Descriptive statistics were calculated to summarize baseline characteristics and primary tumor response. Categorical variables were compared using the chi-squared test or Fisher's exact probability method. The Kaplan – Meier method and log-rank test were applied to estimate the PFS and OS with associated two-sided 95% confidence intervals (CIs). Hazard ratios (HRs) and the associated 95% CIs were calculated using a stratified Cox proportional hazards model. All statistical analyses were performed using GraphPad Prism 8 (GraphPad Software, San Diego, CA, USA) and R software version 4.1.0 (R Project for Statistical Computing). Significance was assumed at $p < 0.05$.

Results

NSCLC patients with diabetes shortens survival period and inhibits CD8^{+} T cells function

Overall, 436 patients with advanced or metastatic NSCLC who received anti-PD-1 immunotherapy as a first-line treatment between November 2018 and December 2021 were enrolled in the study. Demographic and baseline characteristics of the patients are presented in Table 1. Patients with and without diabetes accounted for 16.3% (71/436) and 83.7% (365/436), respectively. The median age was 68 (range: 52–89) and 65 (range: 39–85) years for patients with and without diabetes, respectively. Disease stage, smoking history, comorbidities,

Table 1. Baseline of patients' demographics and clinical characteristics in retrospective cohort.

	All patients ($n = 436$)	Nondiabetic patients ($n = 365$)	Diabetic patients ($n = 71$)	p value
Gender				0.275
Male	393(90.1%)	326(89.3%)	67(94.4%)	
Female	43(9.9%)	39(10.7%)	4(5.6%)	
Median age, years	66.5(39–89)	65(39–85)	68(52–89)	0.438
Disease stage				0.574
IIIb-IIIc	130(29.8%)	111(30.4%)	19(26.8%)	
IV	306(70.2%)	254(69.6%)	52(73.2%)	
Smoking status				0.575
Never smoker	134(30.7%)	110(30.1%)	24(33.8%)	
Smoker	302(69.3%)	255(69.6%)	47(66.2%)	
Comorbidities				0.176
Hypertension	138(31.7%)	108(29.6%)	30(42.3%)	
COPD	142(32.6%)	121(33.2%)	21(29.6%)	
Cerebralcardio vascular diseases	20(4.6%)	15(4.1%)	5(7.0%)	
Coronary artery disease	22(5.0%)	15(4.1%)	7(9.9%)	
Histology				0.585
Adenocarcinoma	193(44.3%)	159(43.6%)	34(47.9%)	
Squamous cell carcinoma	230(52.8%)	196(53.7%)	34(47.9%)	
Poorly-differentiated NSCLC	13(2.9%)	10(2.7%)	3(4.2%)	
PD-L1 expression				0.264
≥50%	51(11.7%)	42(11.5%)	9(12.7%)	
1%-49%	98(22.5%)	76(20.8%)	22(31.0%)	
<1%	141(32.3%)	121(33.2%)	20(28.2%)	
Un-detect	146(33.5%)	126(34.5%)	20(28.2%)	
Immunotherapy regimens				
Monotherapy	35(8.0%)	29(7.9%)	6(8.5%)	0.814
Combination with chemotherapy	401(92.0%)	336(92.1%)	65(91.5)	
Sites of distant metastases at first diagnosis				0.260
Bone	97(22.2%)	81(22.2%)	16(22.5%)	
Lung	65(14.9%)	55(15.1%)	10(14.1%)	
Liver	30(6.9%)	20(5.5%)	10(14.1%)	
Adrenal	25(5.7%)	20(5.5%)	5(7.0%)	
CNS	56(12.8%)	49(13.4%)	7(9.9%)	
Pleura	101(23.2%)	82(22.5%)	19(26.8%)	

CNS: Central nervous system; COPD:Chronic Obstructive Pulmonary Disease.

histology results, immunotherapy regimen, PD-L1 expression, and sites of distant metastases at first diagnosis did not differ significantly between patients with and without diabetes.

We analyzed the ORR, PFS, and OS in patients with or without diabetes. The final follow-up date was November 30, 2023. For the 365 NSCLC patients without diabetes who underwent ICIs therapy as a first-line treatment, 0.3% (1/365) achieved a complete response (CR), 43.3% (158/365) achieved a partial response (PR), 41.4% (151/365) showed stable disease (SD), and 4.7% (17/365) had progressive disease (PD). For 10.4% (38/365) of the patients, data on treatment efficacy were unavailable because patients had postoperative recurrence, and no target lesions were identified for evaluation. Among patients with diabetes, 35.2% (25/71) achieved PR, 53.5% (38/71) showed SD, and 5.6% (4/71) had PD. For 5.6% (4/71) of patients, efficacy evaluation was lacking. The ORR was 43.6% and 35.2% for patients without and with diabetes, respectively. Patients with diabetes showed a shorter PFS than those without diabetes (7.0 vs. 11.0 months). The stratified HR for disease progression or death was 1.5 (95% CI: 1.1–2.0; $p = 0.0069$) (Figure 1a). The OS was 17.0 and 26.0 months in patients with and without diabetes, respectively (HR: 1.5, 95% CI: 1.0–2.1; $p = 0.0122$) (Figure 1b). This indicated that patients with diabetes had worse ORR, PFS, and OS than those without diabetes.

We analyzed T-cells infiltration in 148 patients with NSCLC (121 patients without diabetes and 27 with diabetes). We performed immunohistochemical staining of CD3 and CD8 and found that patients without diabetes had high CD8$^+$ T cells infiltration (Figure 1c). Patients with diabetes had significantly less CD8$^+$ T cells infiltration than patients without diabetes (45.96 vs. 151.9, $p = 0.0374$, Figure 1d). Furthermore, we analyzed PBMCs from 43 patients with NSCLC (16 with diabetes and 27 without diabetes) using flow cytometry to determine the numbers of CD8$^+$ T cells (Figure 1e). The results were consistent with those of human lung tissue. Patients with diabetes had significantly lower percentages of CD8$^+$ T cells than those without diabetes ($np = 0.0299$, Figure 1f). Moreover, the expression of immunosuppressive checkpoints such as PD-1, T-cell immunoreceptor with Ig and ITIM domains (TIGIT), and lymphocyte activation gene-3 (LAG3) were significantly higher in NSCLC patients with diabetes (Figure 1g). The proportion of killer cell lectin-like receptor G1 (KLRG1) and GNLY-positive cells were significantly lower among infiltrating CD8+ T cells in NSCLC with diabetes, and the proportion of GZMB exhibited no significant difference (Figure 1h).

Major peripheral immune components in NSCLC patients with or without diabetes

To investigate the peripheral blood immunological characteristics of patients with or without diabetes, we enrolled 17 patients with advanced NSCLC who received first-line immunotherapy from July 2022 to December 2022. Among these 17 patients, 7 were diabetes and 10 were without diabetes. The clinical characteristics of these patients are shown in Supplementary Table S2. We obtained CyTOF data from the 17 patients at baseline before anti-PD-1 treatment and matched PBMC samples 3 weeks after first-line anti-PD-1 treatment (Figure 2a). After processing the

original file 70,000 cells were obtained from each sample. Thirty-three major immune cell clusters were identified using the classic PhenoGraph clustering method. Based on the canonical cell surface markers, we defined 33 major cell clusters, including 7 of CD4$^+$ T cells (CD3$^+$CD4$^+$), 7 of CD8$^+$ T cells (CD3$^+$CD8$^+$), 2 of B cells (CD3$^-$CD19$^+$), 4 of natural killer cells (NK, CD3$^-$CD56$^+$), 4 of monocytes (CD14$^+$CD86$^+$HLA-DR$^+$), and 8 of other subsets, including γδ T cells (CD3$^+$γδ TCR$^+$), natural killer T cells (NKT, CD3$^+$CD56$^+$), double-positive T cells (DPT, CD3$^+$CD4$^+$CD8$^+$), double-negative T cells (CD3$^+$CD4$^-$CD8$^-$), and dendritic cells (CD11c$^+$HLA-DR$^+$; pDC, CD123$^+$HLA-DR$^+$). The C32 cluster was undefined for lacking classic markers (Supplementary Figure S1A, B). The different marker expression levels of the 33 clusters are shown in Supplementary Table S3. All cell clusters were divided into 13 subsets; CD4$^+$T cells accounted for 29.33%, CD8$^+$T cells accounted for 16.39%, NK cells accounted for 18.3%, and monocytes accounted for 23.15% (Figure 2b, c). We then analyzed the differences in patients with or without DM before and after anti-PD-1 treatment and found evident differences for some cell subsets (Figure 2d). We also compared the proportion of immune clusters in patients with or without diabetes before and after anti-PD-1 treatment, and the results showed that the proportion of immune clusters highly differed among NSCLC patients with diabetes before anti-PD-1 treatment (DMB), NSCLC with diabetes after anti-PD-1 treatment (DMA), NSCLC without diabetes before anti-PD-1 treatment (NDMB), and NSCLC without diabetes after anti-PD-1 treatment (NDMA) (Supplementary Figure S1C). In most patients, CD4$^+$ and CD8$^+$ T cells accounted for the largest proportion. However, NK cells accounted for the largest population of B005. These results indicated tumor heterogeneity among PBMC samples from different patients (Supplementary Figure S1D). Furthermore, we compared the proportion and frequency of immune subsets before anti-PD-1 treatment and 3 weeks after anti-PD-1 treatment between the two groups, but there were no significant differences in DMB, NDMB, DMA, and NDMA patients (Figure 2e). The expression of multiple PBMC-derived immune cell markers in patients with or without diabetes before and after anti-PD-1 immunotherapy is shown in Supplementary Figure S1E-F. The expression of T cell activation and toxicity markers such as CD38, GZMB, and HLA-DR were obviously increased after anti-PD-1 treatment in the group without diabetes.

NSCLC patients with diabetes showed higher CD161$^+$CD127$^+$CD8$^+$ T cells proportions in CD8$^+$T cells

Furthermore, we identified the clusters and distribution of immune cell subsets in CD8$^+$ T cells to compare the differences between patients with or without diabetes before and after anti-PD-1 therapy. 21 clusters of CD8$^+$ T cells were analyzed, including 4 naïve CD8$^+$ T cells (CD45RA$^+$CCR7$^+$), 8 effector memory CD8$^+$ T cells (CD45RA$^-$CCR7$^-$), 6 effector CD8$^+$ T cells (CD45RA$^+$CCR7$^-$), 2 CD161$^+$CD127$^+$CD8$^+$ T cells, and 1 CD57$^+$CD161$^+$GZMB$^+$CD8$^+$ T cell clusters (Figure 3a, b). The expression levels of different markers in the 21 clusters are shown in Supplementary Table S4. The percentage of 21 clusters for immune cell subpopulations in DMB, NDMB, DMA, and NDMA patients were analyzed and shown in Figure 3c. First, we compared the different immune cell clusters between DMB
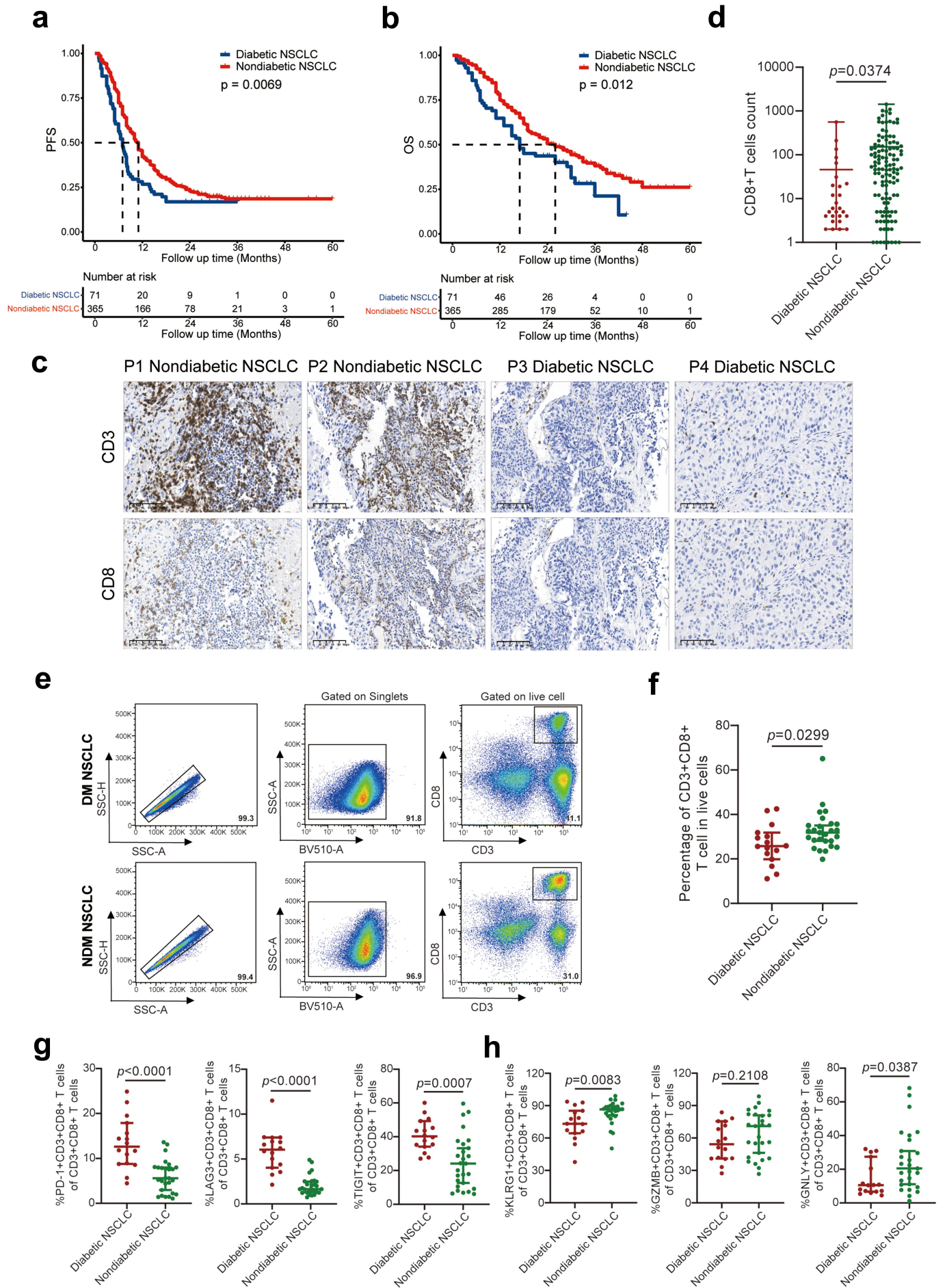
and NDMB patients. Compared to that in NDMB patients, the C01 cluster (CD161$^+$CD127$^+$CD8$^+$ T cells) was evidently increased in DMB patients compared with NDMB patients (p = 0.0071), and this trend was also observed in DMA patients when compared with NDMA patients (p = 0.0393, Figure 3d). Furthermore, we found that at baseline, NDMB patients were more enriched in the C19 cluster (CD57$^+$CD161$^+$GZMB$^+$CD8$^+$ T cells) than DMB patients (p = 0.0149), and this difference was also observed after anti-PD-1 treatment (p = 0.0219, Figure 3e). The functional markers used to identify subpopulations are shown in Figure 3f. Cluster 19 in NDMA patients had higher GZMB expression than that in DMA patients. Additionally, we analyzed the developmental trajectory of CD8$^+$ T cells to explore the developmental trajectory of the C01 and C19 clusters. We found that all CD8$^+$ T cells could be grouped with three developmental states, mainly from naive CD8$^+$ T cells to effector CD8$^+$ T cells. The C01 cluster was in state 1, and the C19 cluster was in state 3 (Figure 3g).

CD161$^+$CD127$^+$CD8$^+$ T cells exhibit capacity for producing immune-exhaustion markers in NSCLC with diabetes

To verify CD161$^+$CD127$^+$CD8$^+$ T cells proportions among CD8$^+$T cells among PBMCs, we prospectively identified an independent validation cohort consisting of 74 patients with advanced NSCLC from July 2022 to September 2023 (38 patients without diabetes and 36 patients with diabetes). The characteristics of these patients are presented in Table 2. Flow cytometry was performed to analyze PBMCs obtained from the validation cohort at baseline (Figure 4a). Patients with diabetes showed evidently higher CD161$^+$CD127$^+$CD8$^+$ T cells/CD8$^+$ T cells ratios than those in patients without diabetes (6.3% vs. 3.9%, p = 0.0059; Figure 4b). However, the percentage of CD57$^+$CD161$^+$GZMB$^+$CD8$^+$ T cells among CD8$^+$ T cells did not significantly differ between the patients with or without diabetes (3.1% vs. 4.4%, p = 0.1813, Supplementary Figure S2A, B). Next, we determined cytotoxic molecule and immune-exhaustion markers production by CD161$^+$CD127$^+$CD8$^+$ T cell subsets in NSCLC with diabetes. We found that CD161$^+$CD127$^+$CD8$^+$ T cells in NSCLC with diabetes were functionally superior to those in NSCLC without diabetes based on the percentage of PD-1 (p = 0.0011), LAG3 (p = 0.0082), and TIGIT (p < 0.0001) (Figure 4c). However, production of the cytotoxic molecules KLRG1 (p = 0.0329), GZMB (p = 0.0387), and GNLY (p = 0.0395) was lower in the CD161$^+$CD127$^+$CD8$^+$ T cell subsets in patients with diabetes than those in patients without diabetes (Figure 4d).

To further determine the infiltration of CD161$^+$CD127$^+$CD8$^+$ T cells among CD8+T cells in patients with NSCLC, we collected formalin-fixed and paraffin-embedded tissues from 64 patients before anti-PD-1 therapy to perform multiplex immunohistochemistry/immunofluorescence testing (34 patients with diabetes

and 30 patients without diabetes). The patients with diabetes had significantly higher infiltration of CD161$^+$CD127$^+$CD8$^+$ T cells/CD8$^+$ T cells than those without diabetes (P=0.0036) (21.4% vs. 12.0%, Figure 4e, f). Simultaneously, we investigated CD57$^+$CD161$^+$GZMB$^+$CD8$^+$ T cell infiltration among CD8$^+$ T cells in patients with and without diabetes (Supplementary Figure S2C). As CD57$^+$CD161$^+$GZMB$^+$CD8$^+$ T cells did not significantly differ in the flow cytometry validation between the patients with and without diabetes, statistical analysis was not performed on the data from the tissue samples.

Transcriptomic analysis revealed differences between CD161$^+$CD127$^+$CD8$^+$ T cells and CD161$^+$CD127$^-$CD8$^+$ T cells in NSCLC with diabetes

To elucidate the molecular mechanisms of CD161$^+$CD127$^+$CD8$^+$ T cells, we conducted RNA-seq using sorted cells from NSCLC patients with diabetes prior to immunotherapy. RNA-bulk analysis showed 88 downregulated and 114 upregulated DGEs in CD161$^+$CD127$^+$CD8$^+$ T cells compared to CD161$^+$CD127$^-$CD8$^+$ T cells respectively (Figure 5a). Clustering analysis of gene expression separated the samples into two clusters: CD161$^+$CD127$^+$CD8$^+$ T cells and CD161$^+$CD127$^-$CD8$^+$ T cells. It further revealed that GZMB, GZMH, GNLY, and KLRD1 were downregulated in CD161$^+$CD127$^+$CD8$^+$ T cells (Figure 5b). This identified DEGs provide novel insights into the molecular characteristics and potential functional roles of CD161$^+$CD127$^+$CD8$^+$ T cells in the context of PD-1 inhibitor treatment of NSCLC patients. Gene Ontology (GO) and Kyoto Encyclopedia of Genes and Genomes (KEGG) analyses were performed to analyze DEG functions. Based on the 88 downregulated DGEs in CD161$^+$CD127$^+$CD8$^+$ T cells, most of the DEGs were associated with immune-related biological process, including natural killer cell-mediated immunity and cytotoxicity (Figure 5c). Subsequently, 88 downregulated DEGs could be annotated using the KEGG database. Based on the KEGG pathway enrichment analyses, DEGs were significantly enriched in natural killer cell-mediated cytotoxicity pathways (Figure 5d). These findings demonstrate the distinctive molecular features and potential functions of CD161$^+$CD127$^+$CD8$^+$ T cells during anti-PD-1 treatment of NSCLC patients with diabetes, which may facilitate future investigations.

CD161$^+$CD127$^+$CD8$^+$ T cells to CD8$^+$T cells ratio is associated with survival outcomes in NSCLC with diabetes

We investigated whether the level of CD161$^+$CD127$^+$CD8$^+$ T cells among CD8+T cells influenced the clinical prognosis of 74 patients with NSCLC. The final follow-up was on November 30, 2023. Flow cytometric analysis revealed that, within CD8$^+$ T cells, the median level of CD161$^+$CD127$^+$ CD8$^+$ T cells in the

Figure 1. NSCLC patients with diabetes shortens survival period and inhibits CD8$^+$ T cells function. (a) Progression-free survival in patients without (n = 365) and with (n = 71) diabetes (11.0 vs. 7.0 months, p = 0.0069). (b) Overall survival in patients without and with diabetes (26.0 vs. 17.0 months, p = 0.0122). (c) Immunohistochemical staining analysis of CD3$^+$ T cells and CD8$^+$ T cells in NSCLC patients with or without diabetes. (d) Patients with diabetes had lower CD8$^+$ T cells infiltration than those without diabetes (p = 0.0374). (e) Flow cytometry analysis of the percentage of CD3$^+$CD8$^+$ T cells in NSCLC patients. (f) Patients with diabetes had a significantly lower percentage of CD8$^+$ T cells than those without diabetes (p = 0.0299). (g) Percentages of immunosuppressive checkpoints secreting PD-1, TIGIT, and LAG3 in CD3+CD8$^+$ T cells are summarized. Unpaired Student's t test (p < 0.001). (H) Percentages of cytokines secreting KLRG1, GNLY, and GZMB in CD3+CD8$^+$ T cells are summarized. Unpaired Student's t test (p < 0.05 except for GZMB). **NSCLC** :non-small-cell lung cancer, P1: Patient 1, P2: Patient 2, P3: Patient 3, P4: Patient 4.
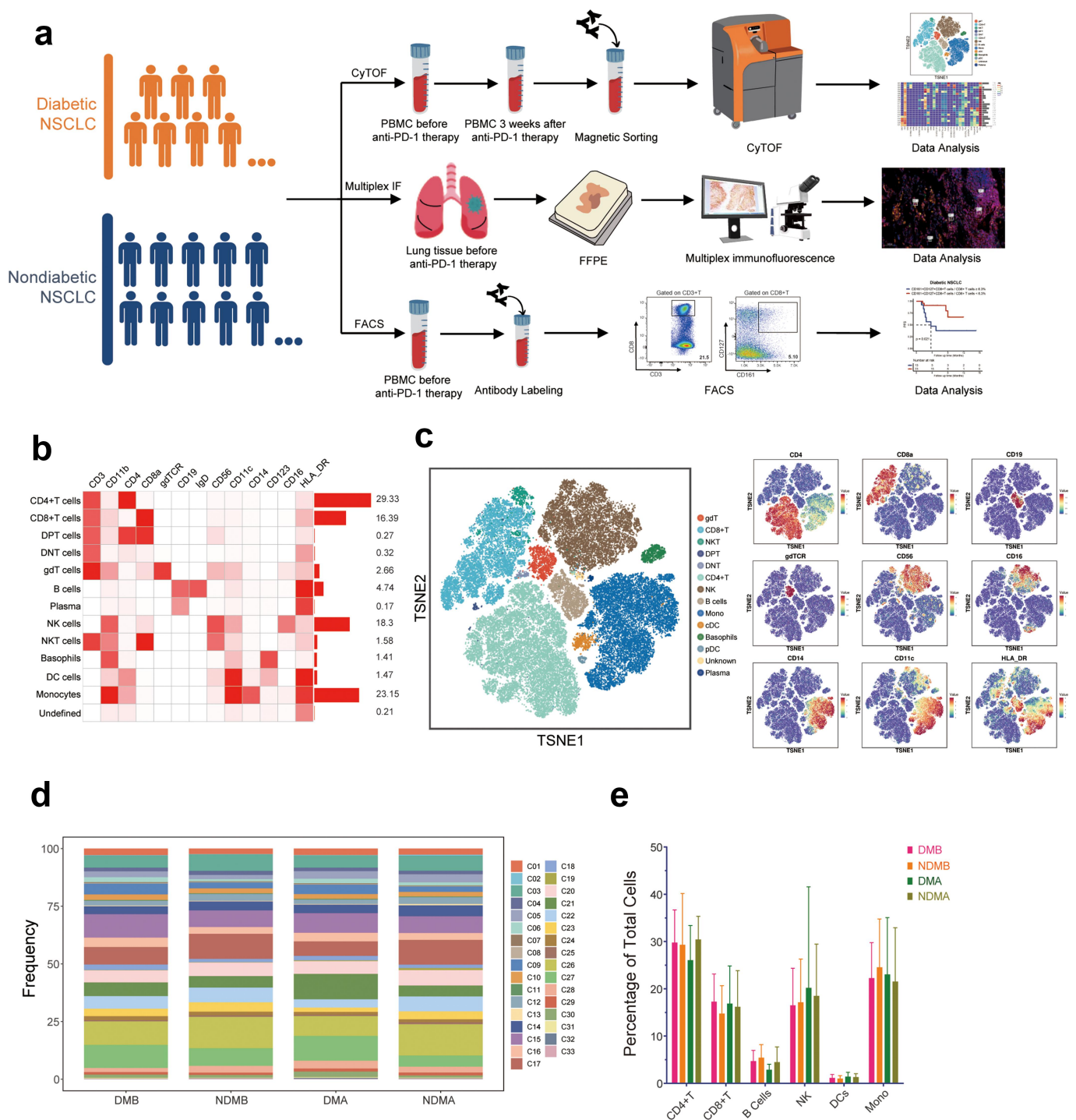
Figure 2. Major peripheral immune components in NSCLC patients with or without diabetes. (a) CyTOF, multiplex IF, and flow cytometry workflow. CyTOF data from 7 patients with diabetes and 10 patients without diabetes at the baseline before anti-PD-1 treatment and matched PBMC samples 3 weeks after first-line anti-PD-1 treatment. Flow cytometry from patients with or without diabetes at the baseline before anti-PD-1 treatment. Multiplex if from patients with or without diabetes at the baseline before anti-PD-1 treatment. (b) Proportion of 13 cell subsets in 33 clusters. (c) Exemplary t-distributed stochastic neighbor embedding plots showed the distribution of all 33 clusters. Signature markers (e.g., CD4, CD19, and CD56) revealed the distribution of immune clusters. (d) Different frequencies of all 33 clusters in DMB, NDMB, DMA, and NDMA patients. (e) Proportion of immune cell subsets in DMB, NDMB, DMA, and NDMA patients. **NSCLC**: non-small-cell lung cancer; **DMB**: NSCLC patients with diabetes before anti-PD-1 treatment. **DMA**: NSCLC patients with diabetes after anti-PD-1 treatment. **NDMB**: NSCLC patients without diabetes before anti-PD-1 therapy. **NDMA**: NSCLC patients without diabetes after anti-PD-1 therapy. **IF**: Immunofluorescence; **CyTOF**: Mass cytometry by time-of-flight. NK: Natural killer cells; NKT: Natural killer T cells; DPT: Double positive T cells; DNT: Double negative T cells; cDCs: Conventional dendritic cells; pDCs: Plasmacytoid dendritic cells.

diabetic patients with metastatic NSCLC was 6.3%, thus this value was used as a cutoff to stratify patients. First, we analyzed PFS in 74 NSCLC patients and found that the differences were insignificant in the $CD161^+CD127^+CD8^+$ T cells to $CD8^+T$ cells ratios ($\geq 6.3\%$ and $< 6.3\%$) between the groups

($p = 0.7243$, Figure 6a). Furthermore, Kaplan–Meier survival analysis showed that patients with diabetes with $CD161^+CD127^+CD8^+$ T cells to $CD8^+T$ cells ratios $\geq 6.3\%(n = 13)$ exhibited shorter PFS than those with $CD161^+CD127^+CD8^+$ T cells to $CD8^+T$ cells ratios $< 6.3\%$
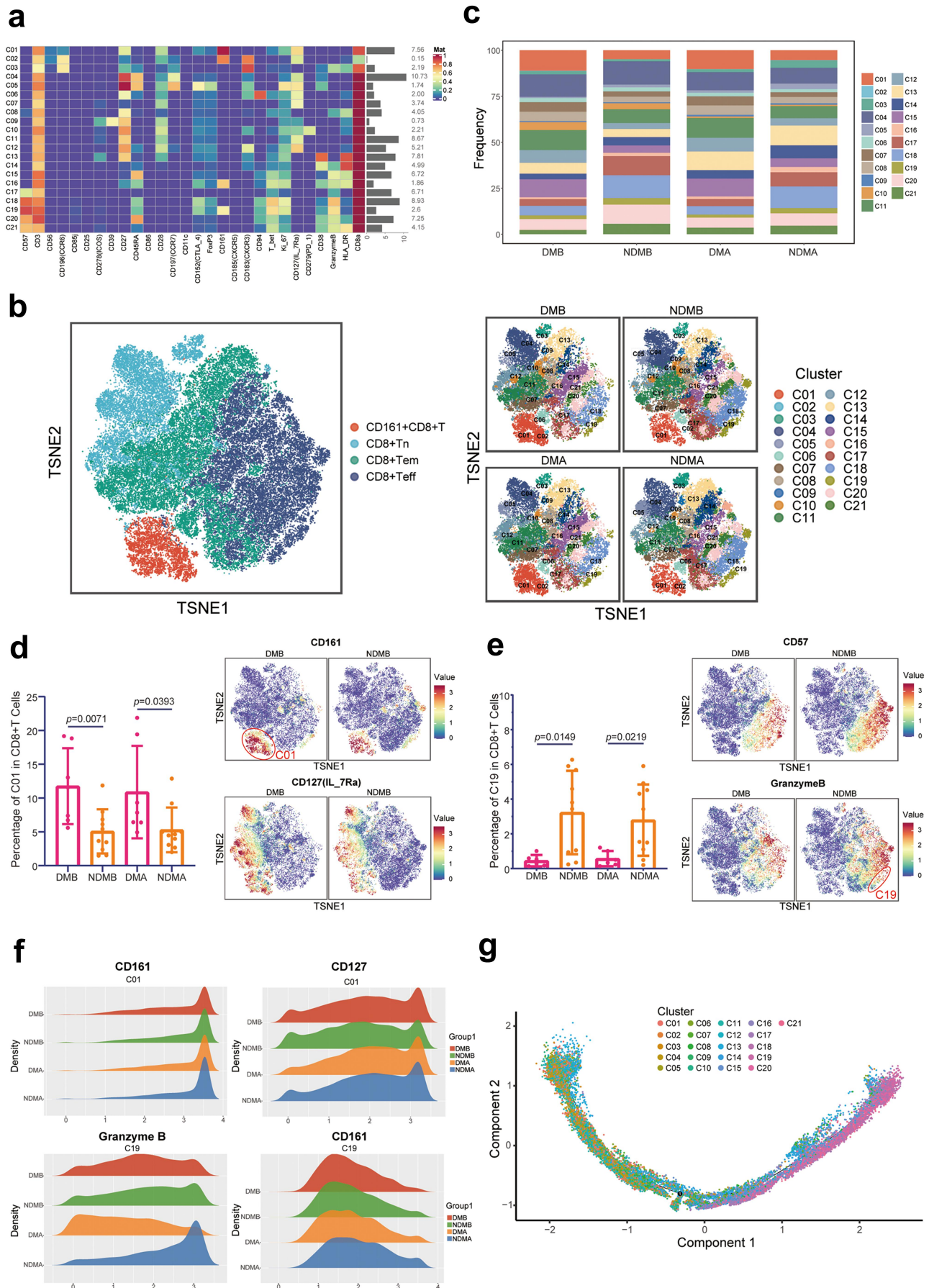
Figure 3. NSCLC patients with diabetes showed higher CD161$^+$CD127$^+$CD8$^+$ T cells proportions in CD8$^+$T cells. (a) Heatmaps showing the distribution of all 21 clusters in CD8$^+$ T cells. (b) T-distributed stochastic neighbor embedding plots showing the distribution of all 21 clusters in DMB, NDMB, DMA, and NDMA patients. (c) Different frequency of all 21 clusters in CD8$^+$ T cells in DMB, NDMB, DMA, and NDMA patients. (d) C01 cluster (CD161$^+$CD127$^+$CD8$^+$ T cells) was significantly increased in patients with diabetes compared to that in those without diabetes before and after anti-PD-1 treatment. (e) C19 cluster (CD57$^+$CD161$^+$GZMB$^+$CD8$^+$ T cells) was significantly

Table 2. The characteristics of patients who received flow cytometry validation.

	All patients (n = 74)	Nondiabetic patients (n = 38)	Diabetic patients (n = 36)	p value
Gender				0.082
Male	65(87.8%)	36(94.7%)	29(80.6%)	
Female	9(12.2%)	2(5.3%)	7(19.4%)	
Median age, years	64.7(44–81)	65.3(44–70)	64.2(46–81)	0.620
Disease stage				
IIIb-IIIc	35(47.3%)	15(39.5%)	20(55.6%)	0.244
IV	39(52.7%)	23(60.5%)	16(44.4%)	
Smoking status				
Never smoker	21(28.4%)	10(26.3%)	11(30.6%)	0.798
Smoker	53(71.6%)	28(73.7%)	25(69.4%)	
Comorbidities				0.366
Hypertension	28(37.8%)	9(23.7%)	19(52.8%)	
COPD	22(29.7%)	12(31.6%)	10(27.8%)	
Cerebralcardio vascular diseases	4(5.4%)	1(2.6%)	3(8.3%)	
Coronary artery disease	6(8.1%)	3(7.9%)	3(8.3%)	
Histology				
Adenocarcinoma	32(43.2%)	13(34.2%)	19(52.8%)	0.175
Squamous cell carcinoma	39(52.7%)	24(63.2%)	15(41.7%)	
Poorly-differentiated NSCLC	3(4.1%)	1(2.6%)	2(5.6%)	
PD-L1 expression				0.090
≥50%	18(24.3%)	11(28.9%)	7(19.4%)	
1%-49%	23(31.1%)	15(39.5%)	8(22.2%)	
<1%	23(31.1%)	7(18.4%)	16(44.4%)	
Un-detect	10(13.5%)	5(13.2%)	5(13.9%)	
Immunotherapy regimens				
Monotherapy	3(4.1%)	1(2.6%)	2(5.6%)	0.610
Combination with chemotherapy	71(95.9%)	37(97.4%)	34(94.4%)	
Sites of distant metastases at first diagnosis				0.392
Bone	16(21.6%)	10(26.3%)	6(16.7%)	
Lung	9(12.2%)	4(10.5%)	5(13.9%)	
Liver	2(2.7%)	2(5.3%)	0(0.0%)	
Adrenal	4(5.4%)	2(5.3%)	2(5.6%)	
CNS	10(13.5%)	8(21.1%)	2(5.6%)	
Pleura	17(23.0%)	8(21.1%)	9(25.0%)	

CNS: Central nervous system; COPD: Chronic Obstructive Pulmonary Disease.

($n = 23$, 3.7 months vs. NR, $p = 0.0212$, Figure 6b). Notably, patients without diabetes with $CD161^+CD127^+CD8^+$ T cells to $CD8^+$T cells ratios ≥ 6.3% ($n = 8$) exhibited longer PFS than those with $CD161^+CD127^+CD8^+$ T cells ratios < 6.3% ($n = 30$, NR months vs. 8.5, $p = 0.0338$, Figure 6c). Kaplan – Meier survival analysis did not show significant changes in OS in patients with $CD161^+CD127^+CD8^+$ T cells to $CD8^+$T cells ratios ≥ 6.3% and < 6.3% because of the short follow-up period (Figure 6d–f). Moreover, the $CD57^+CD161^+GZMB^+CD8^+$ T cell to $CD8^+$ T cell ratio was not related to survival outcomes in patients with diabetes (Supplementary Figure S2D).

Decreased anti-tumor effect of PD-1 blockade in lung cancer mice with diabetes

We established a subcutaneous tumor-bearing mouse model of lung cancer with or without diabetes (Figure 7a) and compared the changes in tumor volume, body weight, and $CD161^+CD127^+CD8^+$ T cells under anti-PD-1 treatment. After intraperitoneal injection of STZ or citrate buffer and

testing of the plasma glucose concentration on day 14, the plasma glucose concentration of mice in the STZ group was much higher than that in the citrate buffer group ($p < 0.001$) (Figure 7b). Anti-PD-1 treatment significantly reduced tumor load and volume in lung cancer mice without diabetes (P=0.021), whereas no significant difference was observed between the anti-PD-1 treatment and control group of lung cancer mice with diabetes (Figure 7c, d, e, f). Moreover, the body weight of the mice did not differ between the anti-PD-1 treatment and control groups in both the diabetes and non-diabetic mice (Figure 7g, h).

In addition, we compared changes in $CD161^+CD127^+CD8^+$ T cells under anti-PD-1 treatment in the tumor-bearing model in C57BL/6 mice and subjected the tumor immune cells to flow cytometry (Figure 7i). In the diabetic group without anti-PD-1 treatment, the distribution of $CD161^+CD127^+CD8^+$ T cells among $CD8^+$ T cells was consistent with our previous results in human samples ($p = 0.0259$, Figure 7j). Following anti-PD-1 treatment, the infiltration of $CD161^+CD127^+CD8^+$ T cells in $CD8^+$ T cells was higher than that of the nondiabetic group (p

decreased in patients with diabetes compared to that in those without diabetes before and after anti-PD1 treatment. (f) Marker density in C01 and C19 clusters. (g) Developmental trajectory of $CD8^+$ T cells to explore the developmental trajectory of C01 and C19 clusters. At node 1, all cells are divided into three states, with state 1 on the left, predominantly consisting of Naïve CD8 T cells, and state 3 on the right, predominantly consisting of Effector CD8 T cells. **NSCLC**: non-small-cell lung cancer; **DMB**: NSCLC patients with diabetes before anti-PD-1 treatment; **DMA**: NSCLC patients with diabetes after anti-PD-1 treatment. **NDMB**: NSCLC patients without diabetes before anti-PD-1 therapy. **NDMA**: NSCLC patients without diabetes after anti-PD-1 therapy. CD8+Tn: Naïve CD8+T cells; CD8+Tem: Effector memory CD8+T cells; CD8+Teff: Effector CD8+T cells.
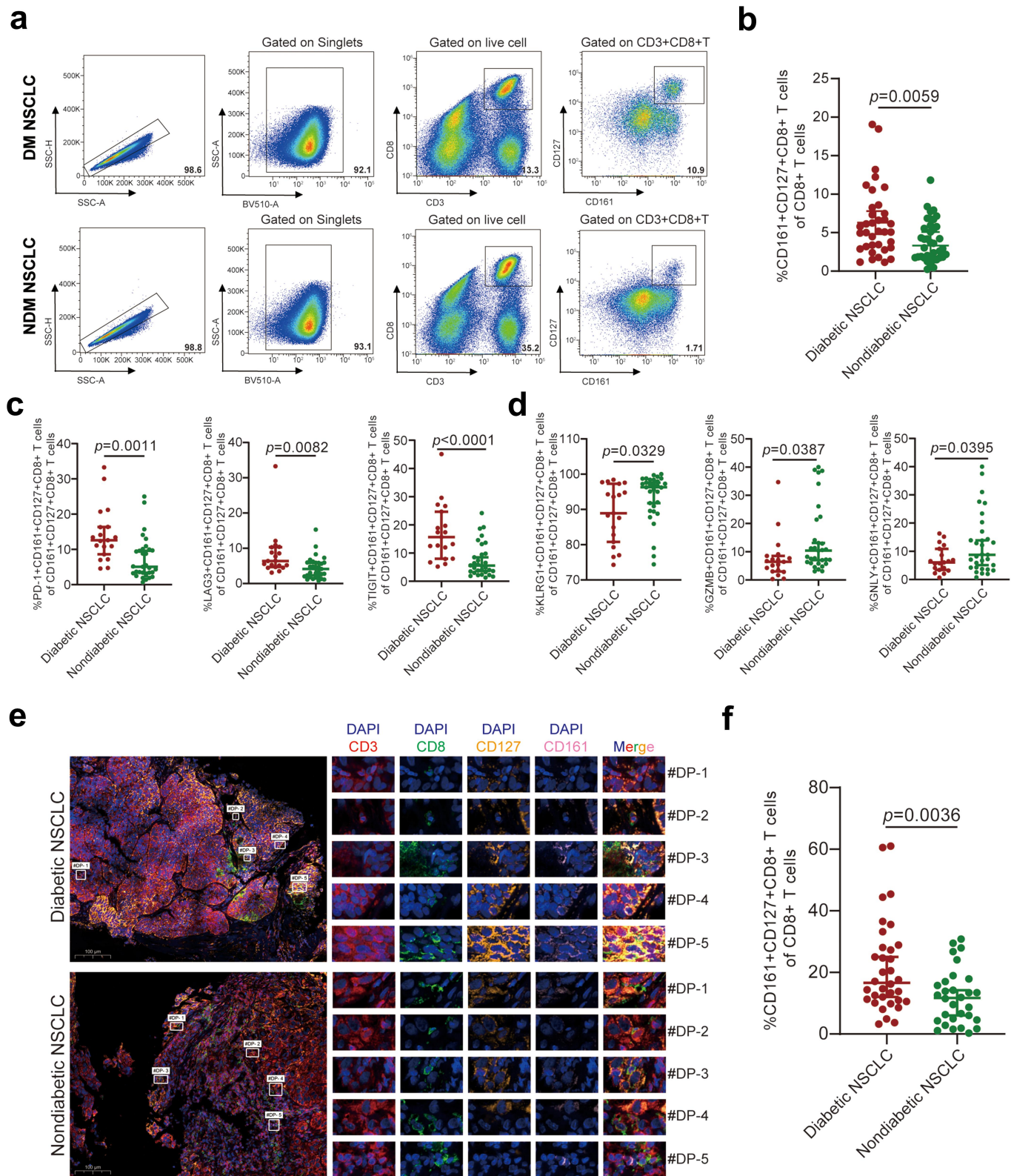
Figure 4. CD161+CD127+CD8+ T cells exhibited capacity for producing immune-exhaustion markers in NSCLC with diabetes. (a) Flow cytometry analysis of CD161+CD127+CD8+ T cells in 74 PBMC samples at baseline before anti-PD-1 treatment. (b) Patients with diabetes ($n = 36$) showed a significantly higher CD161+CD127+CD8+ T/CD8+ T cell ratio than those without diabetes ($n = 38$, 6.3% vs. 3.9%, $p = 0.0059$). (c) Expression of immune-inhibitory receptors in the PBMCs of NSCLC patients with diabetes ($n = 19$) and without diabetes ($n = 31$) via flow cytometry. Unpaired Student's t test ($p < 0.05$). (d) Expression of cytotoxic cytokines in NSCLC patients with diabetes ($n = 19$) and without diabetes ($n = 31$) PBMC via flow cytometry. Unpaired Student's t test ($p < 0.05$). (e) mIHC/IF testing revealed CD161+CD127+ co-expression in CD8+ T cells. (F) Patients with diabetes ($n = 34$) were found to have a significantly higher infiltrate of CD161+CD127+CD8+/CD8+ T cells than those without diabetes ($n = 30$, 21.4% vs. 12.0%, p = 0.0036). **PBMC**: peripheral blood mononuclear cells; **NSCLC**: non-small-cell lung cancer; **mIHC/IF**: multiplex immunohistochemistry/immunofluorescence.
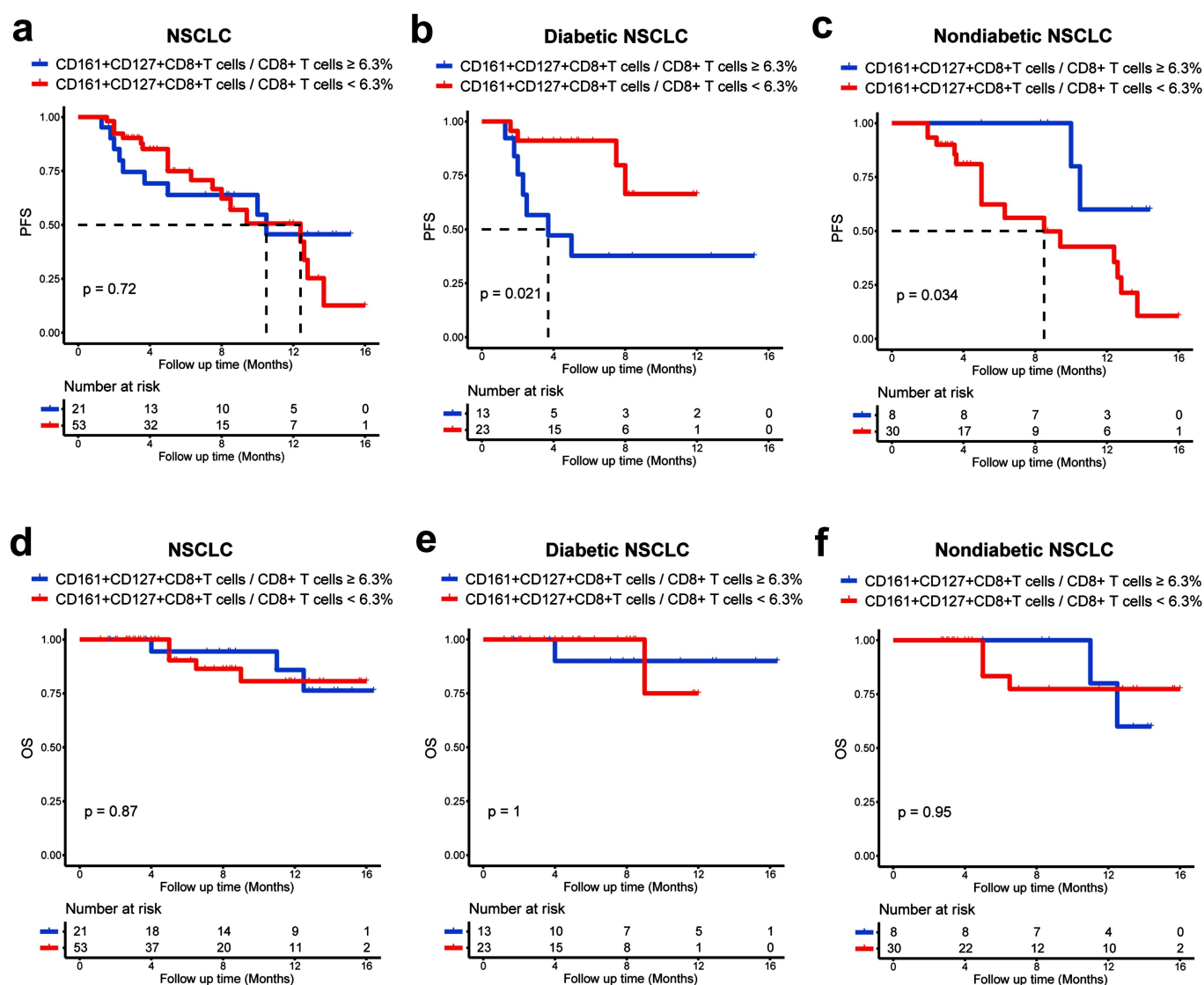
Figure 5. Transcriptomic analysis revealed differences between CD161+CD127+CD8+ T and CD161+CD127−CD8+ T cells in NSCLC with diabetes. (a) Volcano plot showing the 88 downregulated and 114 upregulated DEGs in CD161+CD127+CD8+ T cells compared to CD161+CD127−CD8+ T cells. Red and blue colors represent upregulated and downregulated genes, respectively. (b) Clustering analysis of DEGs and samples. The samples were grouped into two distinct clusters: DP cluster (double positive, CD161+CD127+CD8+ T cells) and CD161 cluster (CD161+CD127−CD8+ T cells). (c) GO analysis of DEGs. The most enriched 30 GO terms in biological process (BP), cellular component (CC), and molecular function (MF). (d) KEGG enrichment analysis of DEGs. The x-axis represents the enrichment score, and the y-axis represents the pathway. **NSCLC**: non-small-cell lung cancer; **GO**: Gene Ontology; **KEGG**: Kyoto Encyclopedia of Genes and Genomes; **DEGs**: differentially expressed genes.

= 0.0067). Notably, this trend was duplicated in peripheral blood immune cell samples from the mouse model (Figure 7i, j). These results indicate that patients and mice with diabetes in lung cancer have enriched CD161+CD127+CD8+ T cells among CD8+ T cells, which is a potential prognostic indicator with poor anti-PD-1 therapeutic effects.

Discussion

Epidemiological evidence indicates that patients with DM have a greater risk of many cancers including breast and pancreatic cancers.[37,38] DM is an independent risk factor for immunotherapeutic resistance during NSCLC treatment.[39,40] Glucose metabolism is vital for the reestablishment of immune cells and changes

Figure 6. CD161+CD127+CD8+ T cells to CD8+T cells ratio is associated with survival outcomes in NSCLC with diabetes. (a) PFS of 74 patients with NSCLC in the CD161+CD127+CD8+ T cells to CD8+ T cells ratio ≥ 6.3% and < 6.3% groups ($p = 0.7243$) based on Kaplan–Meier survival analysis. (b) PFS of 36 NSCLC patients with diabetes in the CD161+CD127+CD8+ T cells to CD8+ T cells ratio ≥ 6.3% and < 6.3% groups ($p = 0.0212$) based on Kaplan–Meier survival analysis. (c) PFS in 38 NSCLC patients without diabetes in the CD161+CD127+CD8+ T cells to CD8+ T cells ratio ≥ 6.3% and < 6.3% groups ($p = 0.0338$) based on Kaplan–Meier survival analysis. (D – F) OS for patients in the CD161+CD127+CD8+ T cells to CD8+ T cells ratio ≥ 6.3% and < 6.3% groups with NSCLC (d), NSCLC and diabetes (e), and NSCLC without diabetes (f) based on Kaplan–Meier survival analysis. **NSCLC**: non-small-cell lung cancer; **PFS**: progression-free survival; **OS**: overall survival.

the tumor microenvironment.[22,41] Recently, Cortellini et al. reported that type 2 DM is an independent risk factor for poor prognosis in patients with advanced cancer receiving immunotherapy, which may be related to the special immunosuppressive state caused by hyperglycemia.[42] However, this cannot clarify the impact of metformin, which is a first-line drug for the treatment of type 2 DM.[43] The tumor microenvironment in patients with NSCLC is affected by DM. In our study, we found that patients with diabetes had worse ORR, PFS, and OS than patients without diabetes who accepted anti-PD-1 immunotherapy as a first-line treatment. Patients with diabetes had higher proportions of CD161+CD127+CD8+ T cells among CD8+ T cells than patients without diabetes before and after anti-PD-1 therapy.

DM can affect lung cancer development and survival through a variety of factors, such as hyperglycemia, hyperinsulinemia, oxidative stress, immune microenvironment, and chronic inflammation associated with cancer progression.[44] Lv et al. found that the serum insulin-like growth factor-1 (IGF-1) level in NSCLC patients with diabetes was significantly reduced, and the IGF-1 metabolic level was a potential indicator for the assessment of cancer risk in patients with DM.[45] Furthermore, hyperglycemia and metabolic dysregulation may result in the growth of lung cancer cells according to epidermal growth factor level, reversal of the Warburg effect, and reactivation of oxidative phosphorylation.[46] Currently, anti-PD-1/PD-L1 immunotherapy is a first-line treatment for patients with advanced non-classical mutated NSCLC.[47,48] In our study, compared with patients without diabetes, patients with diabetes had worse PFS (7.0 vs. 11.0 months, $p = 0.0069$) and OS (17.0 vs. 26.0 months, $p = 0.0122$) after first-line immunotherapy. We aimed to explore why patients with diabetes have a worse prognosis after receiving anti-PD-1 immunotherapy from the perspective of the tumor microenvironment.
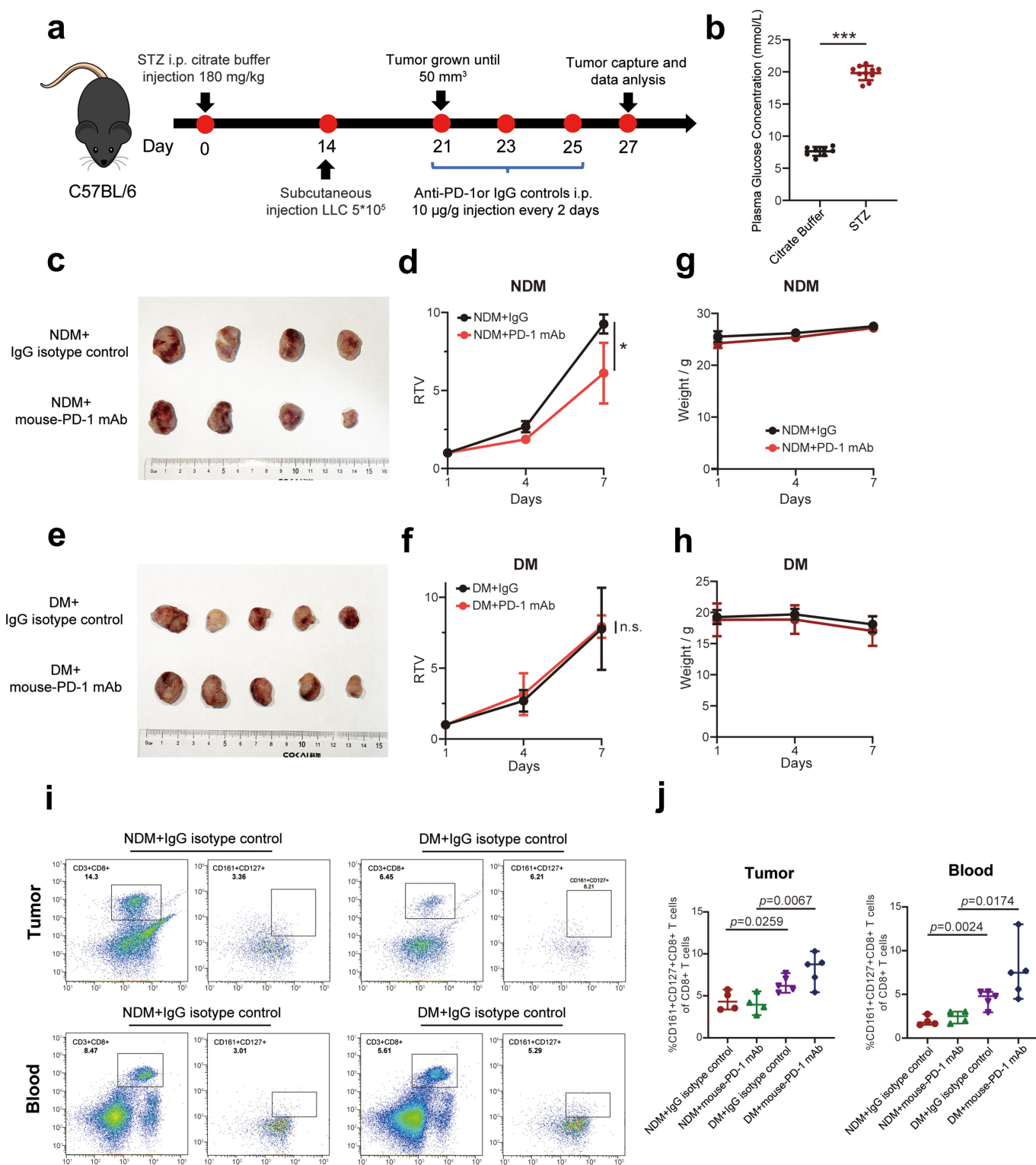
Figure 7. Decreased anti-tumor effect of PD-1 blockade in lung cancer mice with diabetes. (a) Workflow of the animal model. (b) Plasma glucose concentration of mice in both groups tested on day 14. (c) Tumors of mice in NDM group were dissected on day 27. (d) Tumor volume of mice in NDM group was determined every 3 days after anti-PD-1 treatment, and RTV was calculate. (e) Tumors of mice in DM group were dissected on day 27. (f) Tumor volume of mice in DM group was determined every 3 days after the onset of anti-PD-1 treatment, and RTV was calculated. (g) Weight of mice in NDM group was determined every 3 days after anti-PD-1 treatment. (h) Weight of mice in DM group was determined every 3 days after the onset of anti-PD-1 treatment. (i) Flow cytometry of $CD161^+CD127^+CD8^+$ T cells in tumor and peripheral blood under anti-PD-1 treatment in tumor-bearing model C57BL/6 mice. (j) The proportion of $CD161^+CD127^+CD8^+$ T cells among $CD8^+$ T cells was higher in mice with diabetes compared to that in mice without diabetes ($p < 0.05$). **NDM**: Lung cancer mice without diabetes; **RTV**: relative tumor volume; **DM**: Lung cancer mice with diabetes; **mIHC/IF**: multipleximmunohistochemistry/immunofluorescence.

The tumor microenvironment is a complex network comprising cellular and non-cellular elements that play crucial roles in tumor biology, including tumor occurrence, progression, and immune escape.[49,50] Hu et al. compared T cells markers and T cells pool metrics by tumor infiltrating lymphocytes in tumor margins, adjacent lungs, and peripheral blood, and they found that the spatial heterogeneity of the tumor microenvironment in NSCLC significantly affects T cell clonality and T cell diversity, resulting in different anti-tumor immune responses at different lung cancer areas due to differences in the tumor microenvironment.[51] Hyperglycemic metabolism affects cancer proliferation and progression through the remodeling of the tumor microenvironment. Hyperglycemia induces the M2 polarization of tumor-associated macrophages and reduces anti-tumor immunity.[25] Miya et al. found that patients with diabetes had fewer peripheral $CD8^+$ T cells after glucose loading than patients without diabetes.[52] Blood biomarkers can be easily obtained and partly reflect changes in the tumor microenvironment. Moller et al. studied survival-related blood cell parameters in 90 patients with NSCLC who had undergone treatment with ICIs combined with chemotherapy.[53] The authors found that the blood neutrophil count, specific types of monocytes, and the number of blood dendritic cells may be valuable biomarkers for predicting the survival of patients with cancer. In addition to blood markers, the tumor immune microenvironment in PBMCs can reflect the effect of immunotherapy in NSCLC patients with diabetes to a certain extent. Levine et al. used CyTOF to analyze the metabolic phenotypes and cytokine expression profiles of individual $CD8^+$ T cells, and they identified the metabolism of immune cell subsets, which is a valuable way to study the metabolic regulation of immune responses.[54] Wu et al. used CyTOF technology to detect PBMCs in 20 patients and found evident differences in the overall immune status between responses and non-responses patients with intrahepatic cholangiocarcinoma.[55] Patients with higher levels of $CD4^+CXCR3^+$ T cells in PBMCs are more sensitive to gemcitabine-based chemotherapy. In addition, the authors found a strong correlation between the abundance of $CD4^+CXCR3^+$ T cells in PBMCs and the abundance in tumor tissue. This result indicates that the abundance level of PBMCs can indirectly reflect the changes in solid tumor tissue. The present study also used CyTOF to detect PBMCs because this method minimizes the mechanical damage to patients.

In the present study, we discovered differences in the tumor microenvironment between NSCLC patients with or without diabetes before and after anti-PD-1 therapy. Patients with diabetes had lower proportions of $CD8^+$ T cells infiltration and more immune-exhaustion markers than those without diabetes. Compared to those in patients without diabetes, immune- and inflammation-related signaling pathways were suppressed in patients with diabetes. The immune desert state of patients with diabetes implied higher immune cell escape and poorer prognosis. We used CyTOF to further explore the changes in immune cells in the tumor microenvironment at the PBMCs between patients with or without diabetes before and after immunotherapy. Interestingly, the distribution of T cells in the PBMCs was distinct between patients with or without diabetes, especially in clusters 01 ($CD161^+CD127^+CD8^+$ Tcells)

and 19 ($CD57^+CD161^+GZMB^+CD8^+$ T cells), which were both identified as $CD8^+$ T cells. The C01 cluster ($CD161^+CD127^+CD8^+$ T cells) was significantly increased in patients with diabetes, and this trend was also observed after anti-PD-1 treatment. $CD161^+CD127^+CD8^+$ T cells among $CD8^+$T cells may be associated with immunosuppression in patients with diabetes receiving anti-PD-1 treatment. The diagram of $CD161^+CD127^+CD8^+$ T cells in patients with or without diabetes is presented in Supplementary Figure S3.

CD161 is expressed in many immune cells, such as NK cells, $CD4^+/CD8^+$ T cells, and some unconventional T cells such as mucosal-associated invariant T cells, γδT cells, and NKT cells.[56–58] Harms et al. reported that $CD161^+CD8^+$ T cells enhance differentiation in patients with type 1 DM.[59] CD127 expression may be a key indicator of human inflammatory illness[60] and anti-PD-1-treated NSCLC.[48] In the current study, CD161 and CD127 were enriched in patients with diabetes, which is consistent with the results of previous studies. There has been limited research verifying the function of CD161 expression level on $CD8^+$ T cells in tumor immunity in humans, but two different outcomes have been indicated. In a cancer-wide genome analysis of prognostic signatures for gene expressions, killer cell lectin-like receptor subfamily B member 1 (*KLRB1*), the gene encoding CD161, was most frequently related to favorable outcomes against many indications, such as bladder, breast, colon, and prostate cancers, melanoma, lung adenocarcinoma, and multiple myeloma.[61,62] Lao et al. verified a subset of CD161-overexpressing $CD8^+$ T cells abundant in chemo-resistant cancers. The CD161 expression in $CD8^+$ T cells is related to chemoresistance and decreased patient survival rates.[63] However, the role of $CD127^+CD161^+CD8^+$ T cells in NSCLC remains unclear. Some effector $CD8^+$ T cells increase the levels of the IL-7 receptor (CD127) and can differentiate into memory T cells.[64] The activated CD127 can induce precursor B cells during acute lymphoblastic leukemia.[65] Recently, Hui et al. reported that compared to neoadjuvant chemotherapy alone, the combination of anti-PD-1 and neoadjuvant chemotherapy changed the infiltration of immune cells and interactions in patients with NSCLC, reestablishing the tumor immune microenvironment. The authors further showed that the addition of a PD-1 blocker to neoadjuvant chemotherapy facilitated anti-tumor immunity according to the recruitment of T and B cells in the tumor microenvironment and resulted in tumors infiltrating $CD8^+$ T cells to facilitate $CD127^+$ and KLRG 1^+ phenotypes.[66] In our study, $CD161^+$ and $CD127^+$ were both expressed on $CD8^+$ T cells in patients with diabetes, and a high level of $CD127^+CD161^+CD8^+$ T cells among $CD8^+$T cells in patients with diabetes was associated with a worse survival outcome.

Our study has some limitations. First, the results of this study were based only on the analysis of clinical samples, such as peripheral blood and tumor tissues, and have not been thoroughly studied and verified through functional experiments in cells. Second, patients with diabetes received antidiabetic agents (for example metformin), but this factor was not included in this study. Third, other methods, such as spatial transcriptome sequencing of lung cancer tissues, can be added to analyze the interactions between immune cell types of

PBMCs and tumor tissue. Finally, further research with a larger cohort should be conducted to explore the potential use of these methods for predicting and monitoring immunotherapy efficacy in NSCLC patients with diabetes.

Conclusions

Taken together, our results demonstrated that diabetes is a risk factor for NSCLC in patients receiving anti-PD-1 immunotherapy. NSCLC patients with diabetes had worse PFS and OS and showed inhibited $CD8^+$ T cell function compared to those without diabetes. The $CD161^+CD127^+CD8^+$ T cell subset is specifically enriched in NSCLC with diabetes and can produce immune-exhaustion markers. Here, for the first time, we elucidated that $CD161^+CD127^+CD8^+$ T cells may serve as a potential biomarker for predicting the survival outcome of NSCLC patients with diabetes.

Abbreviations

NSCLC	non-small cell lung cancer
CTLA-4	cytotoxic T lymphocyte antigen-4
PD-1	programmed cell death protein 1
PD-L1	programmed cell death protein ligand 1
ERK	extracellular signal-regulated kinase
STAT	signal transducer and activator of transcription
NF	nuclear factor
DM	diabetes mellitus
PFS	progression-free survival
OS	overall survival
mTORC1	mechanistic target of rapamycin complex 1
CyTOF	mass cytometry by time-of-flight
CXCR3	C-X-C chemokine receptor type 3
ORR	objective response rate
PD	progression disease
SD	Stable disease
ICIs	immune checkpoint inhibitors
PBMCs	peripheral blood mononuclear cells
FACS	fluorescence activated cell sorting
PBS	phosphate buffered saline
BSA	bovine serum albumin
KLRB1	killer cell lectin-like receptor subfamily B member 1
HR	hazard ratios
IGF-1	insulin-like growth factor-1

Acknowledgments

Authors' contributions

Availability of data and materials

Data and materials will be made available by the corresponding author upon reasonable request.

Ethics approval and consent to participate

The study was conducted in accordance with the Declaration of Helsinki and was approved by the Institutional Review Board of the First Affiliated Hospital, Zhejiang University School of Medicine (ethical approval number: 2023–0343). All animal experimental procedures were approved by the Ethics Review Committee of the Experimental Animal Center of Zhejiang University School of Medicine (ethical approval number: 2023–974).

Disclosure statement

Funding

ORCID

Jingjing Qu 🆔 http://orcid.org/0000-0002-8079-4722

References

1. Qiu H, Cao S, Xu R. Cancer incidence, mortality, and burden in China: a time-trend analysis and comparison with the United States and United Kingdom based on the global epidemiological data released in 2020. Cancer Commun (Lond). 2021;41(10):1037–1048. doi:10.1002/cac2.12197.
2. Wang M, Herbst RS, Boshoff C. Toward personalized treatment approaches for non-small-cell lung cancer. Nat Med. 2021;27 (8):1345–1356. doi:10.1038/s41591-021-01450-2.
3. Liu SM, Zheng MM, Pan Y, Liu SY, Li Y, Wu YL. Emerging evidence and treatment paradigm of non-small cell lung cancer. J Hematol Oncol. 2023;16(1):40. doi:10.1186/s13045-023-01436-2.
4. Otano I, Ucero AC, Zugazagoitia J, Paz-Ares L. At the crossroads of immunotherapy for oncogene-addicted subsets of NSCLC. Nat Rev Clin Oncol. 2023;20(3):143–159. doi:10.1038/s41571-022-00718-x.
5. Zhu S, Zhang T, Zheng L, Liu H, Song W, Liu D, Li Z, Pan CX. Combination strategies to maximize the benefits of cancer immunotherapy. J Hematol Oncol. 2021;14(1):156. doi:10.1186/s13045-021-01164-5.
6. Wagner G, Stollenwerk HK, Klerings I, Pecherstorfer M, Gartlehner G, Singer J. Efficacy and safety of immune checkpoint inhibitors in patients with advanced non-small cell lung cancer (NSCLC): a systematic literature review. Oncoimmunology. 2020;9 (1):1774314. doi:10.1080/2162402X.2020.1774314.
7. Qu J, Mei Q, Liu L, Cheng T, Wang P, Chen L, Zhou J. The progress and challenge of anti-PD-1/PD-L1 immunotherapy in treating non-small cell lung cancer. Ther Adv Med Oncol. 2021;13:1758835921992968. doi:10.1177/1758835921992968.
8. Wu M, Huang Q, Xie Y, Wu X, Ma H, Zhang Y, Xia Y. Improvement of the anticancer efficacy of PD-1/PD-L1 blockade via combination therapy and PD-L1 regulation. J Hematol Oncol. 2022;15(1):24. doi:10.1186/s13045-022-01242-2.

9. Dora D, Ligeti B, Kovacs T, Revisnyei P, Galffy G, Dulka E, Krizsan D, Kalcsevszki R, Megyesfalvi Z, Dome B. et al. Non-small cell lung cancer patients treated with anti-PD1 immunotherapy show distinct microbial signatures and metabolic pathways according to progression-free survival and PD-L1 status. Oncoimmunology. 2023;12(1):2204746. doi:10.1080/2162402X.2023.2204746.

10. Borderie G, Foussard N, Larroumet A, Blanco L, Domenge F, Mohammedi K, Ducasse E, Caradu C, Rigalleau V. Albuminuric diabetic kidney disease predicts foot ulcers in type 2 diabetes. J Diabetes Complications. 2023;37(2):108403. doi:10.1016/j.jdiacomp.2023.108403.

11. Nanayakkara N, Curtis AJ, Heritier S, Gadowski AM, Pavkov ME, Kenealy T, Owens DR, Thomas RL, Song S, Wong J. et al. Impact of age at type 2 diabetes mellitus diagnosis on mortality and vascular complications: systematic review and meta-analyses. Diabetologia. 2021;64(2):275–287. doi:10.1007/s00125-020-05319-w.

12. Vujkovic M, Keaton JM, Lynch JA, Miller DR, Zhou J, Tcheandjieu C, Huffman JE, Assimes TL, Lorenz K, Zhu X. et al. Discovery of 318 new risk loci for type 2 diabetes and related vascular outcomes among 1.4 million participants in a multi-ancestry meta-analysis. Nat Genet. 2020;52(7):680–691. doi:10.1038/s41588-020-0637-y.

13. Call R, Grimsley M, Cadwallader L, Cialone L, Hill M, Hreish V, King ST, Riche DM. Insulin–carcinogen or mitogen? Preclinical and clinical evidence from prostate, breast, pancreatic, and colorectal cancer research. Postgrad Med. 2010;122(3):158–165. doi:10.3810/pgm.2010.05.2153.

14. Tsilidis KK, Kasimis JC, Lopez DS, Ntzani EE, Ioannidis JPA. Type 2 diabetes and cancer: umbrella review of meta-analyses of observational studies. BMJ. 2015;350(jan02 1):g7607–g7607. doi:10.1136/bmj.g7607.

15. Ramteke P, Deb A, Shepal V, Bhat MK. Hyperglycemia associated metabolic and molecular alterations in cancer risk, progression, treatment, and mortality. Cancers (Basel). 2019;11(9):1402. doi:10.3390/cancers11091402.

16. Saengboonmee C, Seubwai W, Pairojkul C, Wongkham S. High glucose enhances progression of cholangiocarcinoma cells via STAT3 activation. Sci Rep. 2016;6(1):18995. doi:10.1038/srep18995.

17. Pan B, Ren H, Ma Y, Liu D, Yu B, Ji L, Pan L, Li J, Yang L, Lv X. et al. High-density lipoprotein of patients with type 2 diabetes mellitus elevates the capability of promoting migration and invasion of breast cancer cells. Int J Cancer. 2012;131(1):70–82. doi:10.1002/ijc.26341.

18. Giovannucci E, Harlan DM, Archer MC, Bergenstal RM, Gapstur SM, Habel LA, Pollak M, Regensteiner JG, Yee D. Diabetes and cancer: a consensus report. Diabetes Care. 2010;33(7):1674–1685. doi:10.2337/dc10-0666.

19. Su CH, Chen WM, Chen M, Shia BC, Wu SY. Association of diabetes severity and mortality with lung squamous cell carcinoma. Cancers (Basel). 2022;14(10):2553. doi:10.3390/cancers14102553.

20. Lim AR, Rathmell WK, Rathmell JC. The tumor microenvironment as a metabolic barrier to effector T cells and immunotherapy. Elife. 2020;9:e55185. doi:10.7554/eLife.55185.

21. Jia Q, Wang A, Yuan Y, Zhu B, Long H. Heterogeneity of the tumor immune microenvironment and its clinical relevance. Exp Hematol Oncol. 2022;11(1):24. doi:10.1186/s40164-022-00277-y.

22. Zhou T, Hu Z, Yang S, Sun L, Yu Z, Wang G. Role of adaptive and innate immunity in type 2 diabetes mellitus. J Diabetes Res. 2018;2018:1–9. doi:10.1155/2018/7457269.

23. Hu B, Yu M, Ma X, Sun J, Liu C, Wang C, Wu S, Fu P, Yang Z, He Y. et al. IFNalpha potentiates anti-PD-1 efficacy by remodeling glucose metabolism in the hepatocellular carcinoma microenvironment. Cancer Discov. 2022;12(7):1718–1741. doi:10.1158/2159-8290.CD-21-1022.

24. Mu X, Xiang Z, Xu Y, He J, Lu J, Chen Y, Wang X, Tu CR, Zhang Y, Zhang W. et al. Glucose metabolism controls human gammadelta T-cell-mediated tumor immunosurveillance in diabetes. Cell Mol Immunol. 2022;19(8):944–956. doi:10.1038/s41423-022-00894-x.

25. Rodrigues Mantuano N, Stanczak MA, Oliveira IA, Kirchhammer N, Filardy AA, Monaco G, Santos RC, Fonseca AC, Fontes M, Bastos CS Jr. et al. Hyperglycemia enhances cancer immune evasion by inducing alternative macrophage polarization through increased O-GlcNAcylation. Cancer Immunol Res. 2020;8(10):1262–1272. doi:10.1158/2326-6066.CIR-19-0904.

26. Fainsod-Levi T, Gershkovitz M, Vols S, Kumar S, Khawaled S, Sagiv JY, Sionov RV, Grunewald M, Keshet E, Granot Z. Hyperglycemia impairs neutrophil mobilization leading to enhanced metastatic seeding. Cell Rep. 2017;21(9):2384–2392. doi:10.1016/j.celrep.2017.11.010.

27. Kunisada Y, Eikawa S, Tomonobu N, Domae S, Uehara T, Hori S, Furusawa Y, Hase K, Sasaki A, Udono H. Attenuation of CD4(+) CD25(+) regulatory t cells in the tumor microenvironment by metformin, a type 2 diabetes drug. EBioMedicine. 2017;25:154–164. doi:10.1016/j.ebiom.2017.10.009.

28. Zhang Q, Ye M, Lin C, Hu M, Wang Y, Lou Y, Kong Q, Zhang J, Li J, Zhang Y. et al. Mass cytometry-based peripheral blood analysis as a novel tool for early detection of solid tumours: a multicentre study. Gut. 2023;72(5):996–1006. doi:10.1136/gutjnl-2022-327496.

29. Zhang J, Liu T, Duan Y, Chang Y, Chang L, Liu C, Chen X, Cheng X, Li T, Yang W. et al. Single-cell analysis highlights a population of Th17-polarized CD4(+) naive T cells showing IL6/JAK3/STAT3 activation in pediatric severe aplastic anemia. J Autoimmun. 2023;136:103026. doi:10.1016/j.jaut.2023.103026.

30. Eisenhauer EA, Therasse P, Bogaerts J, Schwartz LH, Sargent D, Ford R, Dancey J, Arbuck S, Gwyther S, Mooney M. et al. New response evaluation criteria in solid tumours: revised RECIST guideline (version 1.1). Eur J Cancer. 2009;45(2):228–247. doi:10.1016/j.ejca.2008.10.026.

31. Qu J, Wu B, Chen L, Wen Z, Fang L, Zheng J, Shen Q, Heng J, Zhou J, Zhou J. CXCR6-positive circulating mucosal-associated invariant T cells can identify patients with non-small cell lung cancer responding to anti-PD-1 immunotherapy. J Exp Clin Cancer Res. 2024;43(1):134. doi:10.1186/s13046-024-03046-3.

32. Zunder ER, Finck R, Behbehani GK, E-AD A, Krishnaswamy S, Gonzalez VD, Lorang CG, Bjornson Z, Spitzer MH, Bodenmiller B. et al. Palladium-based mass tag cell barcoding with a doublet-filtering scheme and single-cell deconvolution algorithm. Nat Protoc. 2015;10(2):316–333. doi:10.1038/nprot.2015.020.

33. Finck R, Simonds EF, Jager A, Krishnaswamy S, Sachs K, Fantl W, Pe'er D, Nolan GP, Bendall SC. Normalization of mass cytometry data with bead standards. Cytometry A. 2013;83(5):483–494. doi:10.1002/cyto.a.22271.

34. Levine JH, Simonds EF, Bendall SC, Davis KL, Amir el AD, Tadmor MD, Litvin O, Fienberg HG, Jager A, Zunder ER. et al. Data-driven phenotypic dissection of aml Reveals Progenitor-like Cells that Correlate with Prognosis. Cell. 2015;162(1):184–197. doi:10.1016/j.cell.2015.05.047.

35. van der Maaten L, Hinton G. Visualizing Data using t-SNE. J Mach Learn Res. 2008;9:2579–2605.

36. Qu J, Li M, An J, Zhao B, Zhong W, Gu Q, Cao L, Yang H, Hu C. MicroRNA-33b inhibits lung adenocarcinoma cell growth, invasion, and epithelial-mesenchymal transition by suppressing Wnt/beta-catenin/ZEB1 signaling. Int J Oncol. 2015;47(6):2141–2152. doi:10.3892/ijo.2015.3187.

37. Oldfield L, Evans A, Rao RG, Jenkinson C, Purewal T, Psarelli EE, Menon U, Timms JF, Pereira SP, Ghaneh P. et al. Blood levels of adiponectin and IL-1Ra distinguish type 3c from type 2 diabetes: Implications for earlier pancreatic cancer detection in new-onset diabetes. EBioMedicine. 2022;75:103802. doi:10.1016/j.ebiom.2021.103802.

38. Kim DS, Scherer PE. Obesity, Diabetes, and Increased Cancer Progression. Diabetes Metab J. 2021;45(6):799–812. doi:10.4093/dmj.2021.0077.

39. Lee JY, Jeon I, Lee JM, Yoon JM, Park SM. Diabetes mellitus as an independent risk factor for lung cancer: a meta-analysis of observational studies. Eur J Cancer. 2013;49(10):2411–2423. doi:10.1016/j.ejca.2013.02.025.

40. de Filette JMK, Pen JJ, Decoster L, Vissers T, Bravenboer B, Van der Auwera BJ, Gorus FK, Roep BO, Aspeslagh S, Neyns B. et al. Immune checkpoint inhibitors and type 1 diabetes mellitus: a case

report and systematic review. Eur J Endocrinol. 2019;181(3):363–374. doi:10.1530/EJE-19-0291.

41. Stentz FB, Kitabchi AE. Activated T lymphocytes in Type 2 diabetes: implications from in vitro studies. Curr Drug Targets. 2003;4 (6):493–503. doi:10.2174/1389450033490966.

42. Cortellini A, D'Alessio A, Cleary S, Buti S, Bersanelli M, Bordi P, Tonini G, Vincenzi B, Tucci M, Russo A. et al. Type 2 diabetes mellitus and efficacy outcomes from immune checkpoint blockade in patients with cancer. Clin Cancer Res. 2023;29(14):2714–2724. doi:10.1158/1078-0432.CCR-22-3116.

43. Aroda VR, Knowler WC, Crandall JP, Perreault L, Edelstein SL, Jeffries SL, Molitch ME, Pi-Sunyer X, Darwin C, Heckman-Stoddard BM. et al. Metformin for diabetes prevention: insights gained from the Diabetes prevention program/diabetes prevention program outcomes study. Diabetologia. 2017;60(9):1601–1611. doi:10.1007/s00125-017-4361-9.

44. García-Jiménez C, García-Martínez JM, Chocarro-Calvo A, De la Vieja A. De la Vieja A: A new link between diabetes and cancer: enhanced WNT/β-catenin signaling by high glucose. J Mol Endocrinol. 2014;52(1):R51–R66. doi:10.1530/JME-13-0152.

45. Lv H, Zhang F, Liang C, Liu X, Ma Y, Li J, Ye Y, Si S, Liu Y, Heng H. et al. Decreased IGF-1 level is associated with restrained amino acid metabolism in NSCLC with diabetes mellitus. Front Endocrinol (Lausanne). 2022;13:1031798. doi:10.3389/fendo.2022.1031798.

46. De Rosa V, Iommelli F, Monti M, Fonti R, Votta G, Stoppelli MP, Del Vecchio S. Reversal of Warburg Effect and Reactivation of Oxidative Phosphorylation by Differential Inhibition of EGFR signaling pathways in non-small cell lung cancer. Clin Cancer Res. 2015;21(22):5110–5120. doi:10.1158/1078-0432.CCR-15-0375.

47. Ricciuti B, Wang X, Alessi JV, Rizvi H, Mahadevan NR, Li YY, Polio A, Lindsay J, Umeton R, Sinha R. et al. Association of high tumor mutation burden in non-small cell lung cancers with increased immune infiltration and improved clinical outcomes of PD-L1 blockade across PD-L1 expression levels. JAMA Oncol. 2022;8(8):1160–1168. doi:10.1001/jamaoncol.2022.1981.

48. Caushi JX, Zhang J, Ji Z, Vaghasia A, Zhang B, Hsiue EH, Mog BJ, Hou W, Justesen S, Blosser R. et al. Transcriptional programs of neoantigen-specific TIL in anti-PD-1-treated lung cancers. Nature. 2021;596(7870):126–132. doi:10.1038/s41586-021-03752-4.

49. Goenka A, Khan F, Verma B, Sinha P, Dmello CC, Jogalekar MP, Gangadaran P, Ahn BC. Tumor microenvironment signaling and therapeutics in cancer progression. Cancer Commun (Lond). 2023;43(5):525–561. doi:10.1002/cac2.12416.

50. Petroni G, Buque A, Coussens LM, Galluzzi L. Targeting oncogene and non-oncogene addiction to inflame the tumour microenvironment. Nat Rev Drug Discov. 2022;21(6):440–462. doi:10.1038/s41573-022-00415-5.

51. Hu Q, Frank ML, Gao Y, Ji L, Peng M, Chen C, Wang B, Hu Y, Wu Z, Li J. et al. Spatial heterogeneity of T cell repertoire across NSCLC tumors, tumor edges, adjacent and distant lung tissues. Oncoimmunology. 2023;12(1):2233399. doi:10.1080/2162402X.2023.2233399.

52. Miya A, Nakamura A, Miyoshi H, Takano Y, Sunagoya K, Hayasaka K, Shimizu C, Terauchi Y, Atsumi T. Impact of glucose loading on variations in CD4(+) and CD8(+) T cells in Japanese participants with or without type 2 diabetes. Front Endocrinol (Lausanne). 2018;9:81. doi:10.3389/fendo.2018.00081.

53. Moller M, Turzer S, Ganchev G, Wienke A, Schutte W, Seliger B, Riemann D. Blood immune cell biomarkers in lung cancer patients undergoing treatment with a combination of chemotherapy and immune checkpoint blockade. Cancers (Basel). 2022;14(15):3690. doi:10.3390/cancers14153690.

54. Levine LS, Hiam-Galvez KJ, Marquez DM, Tenvooren I, Madden MZ, Contreras DC, Dahunsi DO, Irish JM, Oluwole OO, Rathmell JC. et al. Single-cell analysis by mass cytometry reveals metabolic states of early-activated CD8(+) T cells during the primary immune response. Immunity. 2021;54(4):829–844 e825. doi:10.1016/j.immuni.2021.02.018.

55. Wu T, Yang Y-C, Zheng B, Shi X-B, Li W, Ma W-C, Wang S, Li Z-X, Zhu Y-J, J-M W. et al. Distinct immune signatures in peripheral blood predict chemosensitivity in intrahepatic cholangiocarcinoma patients. Engineering. 2021;7(10):1381–1392. doi:10.1016/j.eng.2021.01.014.

56. Fergusson JR, Smith KE, Fleming VM, Rajoriya N, Newell EW, Simmons R, Marchi E, Bjorkander S, Kang YH, Swadling L. et al. CD161 defines a transcriptional and functional phenotype across distinct human T cell lineages. Cell Rep. 2014;9(3):1075–1088. doi:10.1016/j.celrep.2014.09.045.

57. Legoux F, Salou M, Lantz O. MAIT cell development and functions: the microbial connection. Immunity. 2020;53(4):710–723. doi:10.1016/j.immuni.2020.09.009.

58. Crosby CM, Kronenberg M. Tissue-specific functions of invariant natural killer T cells. Nat Rev Immunol. 2018;18(9):559–574. doi:10.1038/s41577-018-0034-2.

59. Harms RZ, Lorenzo KM, Corley KP, Cabrera MS, Sarvetnick NE, Fiorina P. Altered CD161 bright CD8+ mucosal associated invariant T (MAIT)-like cell dynamics and increased differentiation states among juvenile type 1 diabetics. PLoS One. 2015;10(1):e0117335. doi:10.1371/journal.pone.0117335.

60. Zhang B, Zhang Y, Xiong L, Li Y, Zhang Y, Zhao J, Jiang H, Li C, Liu Y, Liu X. et al. CD127 imprints functional heterogeneity to diversify monocyte responses in inflammatory diseases. J Exp Med. 2022;219(2):e20211191. doi:10.1084/jem.20211191.

61. Gentles AJ, Newman AM, Liu CL, Bratman SV, Feng W, Kim D, Nair VS, Xu Y, Khuong A, Hoang CD. et al. The prognostic landscape of genes and infiltrating immune cells across human cancers. Nat Med. 2015;21(8):938–945. doi:10.1038/nm.3909.

62. Braud VM, Biton J, Becht E, Knockaert S, Mansuet-Lupo A, Cosson E, Damotte D, Alifano M, Validire P, Anjuere F. et al. Expression of LLT1 and its receptor CD161 in lung cancer is associated with better clinical outcome. Oncoimmunology. 2018;7 (5):e1423184. doi:10.1080/2162402X.2017.1423184.

63. Lao L, Zeng W, Huang P, Chen H, Jia Z, Wang P, Huang D, Chen J, Nie Y, Yang L. et al. CD8+ T cell-dependent remodeling of the tumor microenvironment overcomes chemoresistance. Cancer Immunol Res. 2023;11(3):320–338. doi:10.1158/2326-6066.CIR-22-0356.

64. Wu H, Tang X, Kim HJ, Jalali S, Pritchett JC, Villasboas JC, Novak AJ, Yang ZZ, Ansell SM. Expression of KLRG1 and CD127 defines distinct CD8 + subsets that differentially impact patient outcome in follicular lymphoma. J Immunother Cancer. 2021;9(7):e002662. doi:10.1136/jitc-2021-002662.

65. Almeida ARM, Neto JL, Cachucho A, Euzebio M, Meng X, Kim R, Fernandes MB, Raposo B, Oliveira ML, Ribeiro D. et al. Interleukin-7 receptor alpha mutational activation can initiate precursor B-cell acute lymphoblastic leukemia. Nat Commun. 2021;12(1):7268. doi:10.1038/s41467-021-27197-5.

66. Hui Z, Ren Y, Zhang D, Chen Y, Yu W, Cao J, Liu L, Wang T, Xiao S, Zheng L. et al. PD-1 blockade potentiates neoadjuvant chemotherapy in NSCLC via increasing CD127(+) and KLRG1(+) CD8 T cells. NPJ Precis Oncol. 2023;7(1):48. doi:10.1038/s41698-023-00384-x.